63-3-4

10

[redacted]

403 536

MARKS POLARIZED CORPORATION

THE CONVERSION OF HEAT TO ELECTRICAL POWER BY MEANS OF A CHARGED AEROSOL

Final Report

Period: 1 February 1962 through 4 August 1962

Issued 22 April 1963

Prepared Under: Department of the Navy
Bureau of Naval Weapons
Washington 25, D.C.

Contract NOw 62-0644-c

Marks Polarized Corporation
153-16 Tenth Avenue
Whitestone 57, New York

ABSTRACT

A new process called the condensation aerosol method for the production of small, charged aerosol particles has been developed for use in the electrohydrodynamic energy conversion process. Using this concept, several generators may be placed in series, each one using the same vapor for aerosol formation as the previous unit. Power densities as high as 30 watts/cm^2 of nozzle throat area have been obtained with a single stage condensation aerosol type EHD generator.

Studies of the aerodynamic behavior of the EHD generator with and without energy extraction were made on a fully instrumented test bench. Measurements of the overall efficiency of the generator including frictional losses were made and are reported herein. The kinetic to electric power conversion efficiency of the generator itself was as high as eighty-five percent.

Efforts were made toward designing and building a closed loop system for the generator. A small compressor system for circulating a gas in a closed loop was tested. Calculations were made for the design of a small boiler system for operating a closed loop steam cycle at a few atmospheres pressure.

TABLE OF CONTENTS

TABLE OF CONTENTS - Cont'd

LIST OF ILLUSTRATIONS

LIST OF ILLUSTRATIONS - Cont'd

I INTRODUCTION

The electrohydrodynamic process for the conversion of heat to electrical power starts with the production of small charged aerosol particles in a gas stream whose kinetic energy has been obtained from a heat reservoir. These charged aerosol particles are then caused to do work against an opposing electric field produced by the accumulation of charged particles on a suitable collector. The kinetic energy, hence thermal energy of the gas stream, therefore, is simply converted into usable electrical energy. The EHD generator does not contain any moving parts or large, bulky magnets; thus, high power to weight ratios as well as negligible maintenance are inherent in the EHD generator.

Under the previous research contract[1], the electrojet technique for the simultaneous charging and production of aerosol particles was developed. It was with this type of unit that the first experimental proof of the electrohydrodynamic energy conversion process was obtained. A net electrical power gain of a few milliwatts was obtained.

Previously, the high voltage power supply was connected to the corona point and the charging plate was grounded. It was found in this case that the input current to the generator was always greater than the output current of the unit. When the electrical circuit for the generator was modified by placing the charging plate at high voltage, and then grounding the corona point, the input current was greatly reduced to the point at which it was less than 1% of the output current. With the new configuration, the power supply has only to provide a small amount

of leakage current; thus, the input power is greatly reduced. The maximum output obtained from a generator employing an electrojet type of aerosol production device was about 300 milliwatts.

In the early EHD generator utilizing the electrojet concept, the region between the collector and the charging plate was not enclosed. Since the end result must be a generator which will perform in a closed cycle system, efforts were made to enclose this region. At first, hollow lucite sections of various shapes were inserted between the collector and the charging plate. Preliminary experiments resulted in a thin conducting liquid film formed by the condensation and deposition of the aerosol particles upon the enclosure walls. This film caused current leakage between the collector and the charging plate. The lucite parts were replaced by components made of Teflon which has anti-wetting properties. The only effect this material had was to change the conducting path from a continuous liquid film to a series of droplets.

Measurements were made of the size of the aerosol particles by introducing a silicone oil coated glass slide into the aerosol stream and then photographing it. The sample droplets indicated that the average radius of the aerosol particles was about 5 microns. This large particle size may have been the principle cause of the water deposition on the walls of the enclosure.

A study was undertaken to produce smaller aerosol particles. One method which resulted in submicron particles was to produce the aerosol by condensation of a saturated liquid in the throat

of the nozzle. This was accomplished by injection of a small quantity of liquid into the air stream well upstream of the nozzle. In this manner, the distance for evaporation of the liquid particles and good mixing of the gas streams before the nozzle throat is reached is sufficient. On expanding in the nozzle, the saturated mixture undergoes a temperature drop which causes the mixture to become supersaturated. A corona field produced between the corona point and the charging plate provides ions to act as condensation centers for the vapor to condense upon and charge the droplets.

On very humid days, a thin conducting liquid film formed on the enclosure between the charging plate and the collector. It was found that on damp days, the air contained a sufficient amount of moisture, even after compression, to operate the unit without the injection of additional liquid. On extremely humid days (with high outdoor temperatures), however, a conducting film rapidly formed even without the injection of liquid.

A large filter containing approximately 20 pounds of silica gel was inserted into the air line at a point between the compressor and the generator in order to dry the air before it entered the generator. This filter was sufficient to give several hours of dry air for testing purposes.

The liquid was injected from a small high pressure reservoir, from which the flow was controlled by a fine metering valve and measured with a small liquid flow meter. Various liquids such as water, acetone, or ethyl alcohol were evaluated in the dry air tests.

An instrumented test unit was then built to fully understand the mechanism of generator operation. Instrumentation was provided for the measurement of air flow, temperature, and total and static pressure at various stations throughout the test unit. Rotameters installed upstream of the generator, measured the air flow rate. Instrument housing sections, installed in the air line upstream and downstream of the generator, measured total pressure, static pressure, and temperature changes across the generator. Thus, sufficient data was obtained to analyze the aerodynamic and thermodynamic behavior of the system.

From standard aerodynamic considerations and the data taken, the Mach number at the throat of the nozzle was determined. The experimental results indicated that the maximum electrical output was obtained with sonic flow conditions at the nozzle throat. The output fell off sharply at lower Mach numbers.

A maximum net electrical power output of 2.25 watts was obtained using a 3mm diameter nozzle under sonic conditions and 120 psig inlet pressure.

Neglecting frictional losses, the electrohydrodynamic conversion efficiency (i.e., kinetic to electrical energy conversion efficiency) was measured to be as high as 82%. The overall cycle efficiency was less than 1% as would be expected for open cycle testing.

A feasibility study of series operation of the generator was conducted with the condensation aerosol. It was found that

aerosol particles collected in the first stage would reevaporate and recondense in the second stage to produce the aerosol for this stage. Thus, it may be possible to design a series generator whereby liquid injection is required only in the first stage. The output of the second stage of the 2-stage generator used for the evaluation was only a small fraction of the first stage output. The large pressure drop in the first stage, which resulted in a low inlet pressure to the second stage, was the principal contributing factor to the low output of the second stage.

II THEORETICAL ANALYSIS

A. List of Symbols

- A - area (m^2)
- α - slippage coefficient
- β - system temperature ratio
- C - velocity of sound (m/sec)
- c_p - specific heat at constant pressure (joules/kg °K)
- $d(\Delta P)$ - pressure drop due to electrical energy conversion (Newtons/m^2)
- δ - mass density (kgs/m^3)
- e - electronic charge (coulombs)
- η - viscosity coefficient for gas (kgs/m sec)
- η_c - conversion efficiency
- η_g - generator efficiency
- η_{ov} - overall efficiency
- η_p - pump efficiency
- H - enthalpy (Joules)
- k - particle mobility (m/sec)/(volt/m)
- λ - average mean free path of gas molecules (meters)
- λ_A - average mean free path of gas molecules at atmospheric pressure (meters)
- m - mass (kg)
- M - mass flow (kgs/sec)
- n - aerosol concentration ($particles/m^3$)

N - number of elementary charges per droplet

w_i - work ratio

P - static pressure (Newtons/m^2)

$P_{D.H.}$ - dynamic head pressure (Newtons/m^2)

P_T - total pressure (Newtons/m^2)

P_{out} - cutput electrical power (watts)

P_{in} - input electrical power (watts)

φ - system pressure ratio

r - radius of droplet (meters)

r_μ - radius of droplet (microns)

ρ - charge density in coulombs/meter^3

V - velocity (m/sec)

X - breakdown electric field (volts/m)

X_A - breakdown electric field at atmospheric pressure (volts/m)

B. The Electrohydrodynamic Energy Conversion Process

1. Energy Conversion Analysis

The electrohydrodynamic energy conversion process is the process by which charged aerosol particles are caused to do work against an opposing electric field by means of a moving gas stream. The charged aerosol particles are produced within a moving gas stream whose stagnation enthalpy is:

$$H_1 = mc_pT_1 + mU_1^2/2 \tag{1}$$

The charged aerosol stream then flows into a region in which there is an opposing electric field and flow energy of the stream is extracted and converted to electrical energy. The enthalpy of the air stream after the charged aerosol particles are collected is:

$$H_2 = mc_pT_2 + mU_2^2/2 \tag{2}$$

The enthalpy change in the gas stream is just that which goes into the electrical energy conversion.

$$H_2 - H_1 = mc_p(T_1 - T_2) + m(U_1^2 - U_2^2)/2 \tag{3}$$

The time rate of change of energy or the power developed with constant mass flow M is:

$$P_{Tot} = Mc_p(T_1 - T_2) + M(U_1^2 - U_2^2)/2 \tag{4}$$

which is equal to the theoretical electrical power output of the generator. A measurement of the ratio between the measured electrical output power, and the enthalpy change defines the efficiency of the process.

2. Efficiency

a. Generator Cycle Efficiency. In a closed cycle, the operation of the EHD generator will have to be considered as a single component in a sequence of operations. Therefore, the efficiency of other components in the cycle will have to be considered along with the efficiency of the generator. The overall efficiency of the system may be separated into two portions:

1) Ideal cycle efficiency, η_i.

2) Generator efficiency, η_g.

The ideal cycle efficiency assumes that the generator itself is 100% efficient. The product of the two gives us the overall efficiency, η_{ov}. The efficiencies are defined as follows:

$$\text{Ideal Cycle Efficiency } (\eta_i) = \frac{\text{Isentropic Generator Work}}{\text{Actual Pump Work + Heat Added}} \quad (5)$$

$$\text{Generator Efficiency } (\eta_g) = \frac{\text{Generator Output}}{\text{Isentropic Generator Work}} \quad (6)$$

$$\text{Overall Efficiency } (\eta_i \eta_g) = \frac{\text{Generator Output}}{\text{Actual Pump Work + Heat Added}} \quad (7)$$

Also, another parameter called Ideal Work Ratio is defined as follows:

$$\text{Ideal Work Ratio } (w_i) = \frac{\text{Isentropic Generator Work}}{\text{Pump Work}} \quad (8)$$

The ideal work ratio should be as close to one as possible so that power losses in the system are kept small.

A schematic diagram of the closed cycle is shown in figure 1. The temperature-entropy diagram for the system is shown in figure 2. The subscript i in figure 2 denote the values occurring if the process were isentropic.

From figure 2, we may write the ideal cycle efficiency as:

$$\eta_i = c_p(T_2 - T_{3i})/(c_p(T_1 - T_0) + c_p(T_2 - T_1) \qquad (9)$$
$$= (T_2 - T_{3i})/(T_2 - T_0)$$

Pump efficiency η_p, may be defined in the same manner as generator efficiency to give:

$$\eta_p = c_p(T_{1i} - T_0)/c_p(T_1 - T_0) \qquad (10)$$
$$= (T_{1i} - T_0)/(T_1 - T_0)$$

Combining equations (10) and (9), we obtain:

$$\eta_i = (1 - 1/\beta)/(1 - 1/\tau D) \qquad (11)$$

Where:

$$\beta = \text{system temperature ratio} \qquad (12)$$
$$= T_{1i}/T_0 = T_2/T_{3i}$$
$$\tau = T_2/T_1$$
$$D = 1 + (\beta - 1)/\eta_p$$

Equation (11) can be plotted in terms of system pressure ratio by simply using the relationship between system temperature ratio β, and pressure ratio φ, $(=P_1/P_0)$ for an isentropic process:

$$\beta = \varphi^{(\gamma - 1)/\gamma} \qquad (13)$$

When equation (13) is substituted into equation (11), the ideal cycle efficiency η_i may be plotted as a function of temperature ratio for various values of the pressure ratio φ. This is plotted in figure 3, assuming η_p is equal to 0.8. It

is easily seen from the curve that the ideal cycle efficiency η_i decreases with heating (increased).

However, the ideal work ratio w_i increases with heating:

$$w_i = (T_2 - T_{3i})/(T_1 - T_0) = \tau D \eta_p / \beta \qquad (14)$$

If our EHD generator is to be used as an auxiliary power unit, the ideal cycle efficiency is not of principle importance. The ideal work ratio is the parameter which governs the pump requirements and this is the primary consideration in determining the generator's limitation for this application. The pump requirements decrease with increasing ideal work ratio.

b. Generator Efficiency. The generator efficiency, η_g, takes into account both the frictional power losses and the electrical power conversion losses. The efficiency of the conversion process (i.e., kinetic to electrical energy), neglecting frictional losses, may be determined by experimental means. For a small percentage of energy conversion the conversion efficiency is defined as:

$$\eta_c = (P_{out} - P_{in})/U_n A d(\Delta p) \qquad (15)$$

Where $(P_{out} - P_{in})$ is the net electrical power gain, U_n is the average velocity of the gas in the conversion region, A is the area of the throat, and $d(\Delta P)$ is the total pressure drop across the generator due to only the electrical power conversion process. $d(\Delta P)$ is the so-called electrodynamic effect.

This conversion efficiency parameter is of great importance in evaluating the feasibility of the EHD concept. Experimentally, an efficiency of 85% was measured. This value

indicated that the losses, other than aerodynamic, are small and high generator converter efficiencies can be obtained with a generator unit designed for minimum frictional losses.

C. Charged Aerosol Particle Formation

1. The Electrojet Technique

The electrojet method for the simultaneous production and charging of aerosol particles is shown in figure 4. Liquid, under pressure, is stored in a small reservoir and then fed into the hollow needle which also serves as the corona point. An electric field is set up in the region between the corona point and the charging plate. A surface charge density is induced upon the surface of the liquid as shown in figure 4-A. The air flow and the electric field cause the liquid meniscus to break away since the droplets overcome surface tension forces, as shown in figure 4-C. Highly charged droplets are thus formed.

Because of its high charge, the droplet breaks up during or soon after its formation to form many smaller droplets. However, the particle size distribution is not uniform and the larger droplets formed caused wetting of the surface enclosing the generator.

2. Condensation Aerosol Technique

Further investigation of the surface wetting problem encountered with the electrojet technique resulted in the development of a new method; the condensation aerosol.

In this method, small amounts of liquid are injected through a fine metering valve into the air stream, well upstream

of the generator. Most of the liquid vaporizes and mixes with the air stream by the time it reaches the generator.

The air-vapor stream then expands through the convergent portion of the generator. The resulting temperature drop causes the air to approach its dew point temperature, i.e., saturation point. At the nozzle throat, a corona field is maintained between a corona point and the charging plate which forms the throat of the nozzle. The ions produced by the corona discharge serve as condensation centers for the saturated or near saturated air vapor mixture. The charged aerosol particles produced are sufficiently small so as not to cause wetting of the walls of the enclosure between the charging plate and the collector.

D. Particle Radius as a Function of Pressure, Charge per Particle, and Critical Mobility

A theoretical analysis interrelating mobility, particle radius, charge per particle, and pressure was made. As the starting point, the first requirement to be met is the condition for negligible slip or frictional loss.

$$\alpha = kX/U = 0.01 \tag{16}$$

This may be rewritten in the form:

$$k = \alpha U/X \tag{17}$$

To equation (17) is added the fact that the maximum field strength can be taken as a linear function of pressure in the range of consideration up to 20 atmospheres.

$$X = X_A P_A \tag{18}$$

When equation (18) is combined with equation (19), we obtain:

$$k = \alpha U / X_A P_A \tag{19}$$

We know that at one atmosphere $k = k_A$, so that for the case of sonic velocity $U = C$, at constant temperature we obtain:

$$k_A = \alpha C / X_A \tag{20}$$

$$k = \alpha C / X_A P_A$$

$$k = k_A / P_A \tag{21}$$

The mobility equation is:

$$k = (Ne / 6\pi\eta r)(1 + 0.87\lambda / r) \tag{22}$$

The equation for mean free path as a function of pressure is:

$$\lambda = \lambda_A P_A \tag{23}$$

where λ_A is the mean free path at one atmosphere.

Combining equations (21), (22), and (23), we then solve for r:

$$r = [\lambda_A (0.87) N P_A / 4Y][1 + \sqrt{1 + 8Y / N P_A^2}] \tag{24}$$

$$Y = (.3)(0.87)\pi k_A \lambda_A \eta / e \tag{25}$$

We now evaluate Y, assuming η is constant with pressure:

$e = 1.6 \times 10^{-19}$ coulombs

$k_A = 10^{-6}$ m^2/volt-sec for 1% slip at 1 atmosphere pressure

$\lambda_A = 6.5 \times 10^{-8}$ meters at 1 atmosphere

$\eta \approx 2.5 \times 10^{-5}$ kg/m.sec. units at 1 atmosphere

These values substituted into (25) yield:

$$Y = 83.2$$

Substituting this value into equation (24) we obtain as a final result for our analysis:

$$r = 1.7 \times 10^{-10} NP_A \left(1 + \sqrt{1 + 666/NP_A^2}\right) \tag{26}$$

or

$$r_\mu = 1.7 \times 10^{-4} NP_A \left(1 + \sqrt{1 + 666/NP_A^2}\right)$$

Equation (26) is presented graphically in figure 5 for various values of N. By using equation (26) and the equations of mass continuity and current, we can determine the average radius, particle concentration, and the average charge per droplet. The equations for mass continuity and current are:

$$M_{liq} = n(4/3)\pi r^3 \delta_{liq} AU \tag{27}$$

$$I = \rho AU = nNqAU \tag{28}$$

Since I, A, U, W_{liq}, and P_A may be experimentally measured, we then have three equations in three unknowns, r, n, N. W_{liq} is the mass flow of the liquid injected into the air stream, and n is the particle concentration per unit volume.

E. Closed Cycle Design Studies

1. Air Compressor Cycle

A schematic diagram of an air compressor loop is shown in figure 6. The following conditions are fixed:

a. The area of the throat should be 1 square inch.

b. The static pressure at the throat should be 100 psia.

c. The air velocity at the throat should be sonic.

The mass flow through the system will now be calculated assuming an inlet temperature to the nozzle of 100° F.

$$M_* = \delta_* A_* U_* \tag{29}$$

$$\delta_* = P_*/RT_* \tag{30}$$

$$T_* = .83T_0 \tag{31}$$

$$U_* = \sqrt{\gamma g R T_*} \tag{32}$$

$$P_* = .53P_0 \tag{33}$$

where the subscript (*) refers to the conditions at the nozzle throat and the subscript (0) refers to those at the nozzle inlet.

The symbols used are as follows:

δ - density

T - total temperature

P - static pressure

U - velocity

M - weight flow of air

A - the area

The values of the constants used in these equations are:

$$T_0 = 100°F = 560°R \tag{34}$$

$P_* = 100$ psia $= 14{,}400$ psfa

$A_* = .007$ ft^2

$\gamma = 1.4$

Using the values (34), the results obtained are:

$$P_0 = 189 \text{ psia} = 1.33 \times 10^5 \text{ Newtons/m}^2 \tag{35}$$

$T_* = 466°R = -14.4°C$

$\delta_* = .58$ lb/ft^3 $= 9.28$ kg/m^3

$M_* = 4.25$ lb/sec $= 1.85$ kg/sec

Table I

OPERATING CONDITIONS FOR CLOSED CYCLE AIR COMPRESSOR SYSTEM

Nozzle Throat Diameter (mm)	28.7
Throat area (mm^2)	645
Mach No. at Throat	1
Static Pressure at Throat (psia)	100
Total Pressure at Inlet (psia)	189
Mass Flow (kg/min)	111
Throat Temperature (°C)	-14.4

Estimates[3] were made of the pressure drops which would be encountered throughout the system as follows:

a. Nozzle: zero electric load — 16-26 psi
full electric load — 90 psi

b. Pipe: 3 in. diameter — 5 psi
6 in. diameter — 0.6 psi

The estimate of the pressure drop with full electric load is based on the fact that with a static pressure of 100 psia at the throat of the nozzle, the dynamic head pressure would be 90 psia:

$$P_{D.H.} = P_T(1/.53 - 1) \tag{37}$$

This assumes that the gas will have zero velocity when it leaves the generator and that almost all of the energy of the gas stream has been converted to electrical energy while the remaining energy is consumed by frictional losses. This would mean an extraction of almost 100 kilowatts from the gas stream.

The compressor requirements are therefore:

Inlet pressure	≈ 100 psia
Outlet pressure	≈ 200 psia
Weight flow	≈ 4.25 lb/sec

A 150-horsepower compressor would meet these requirements.

2. Steam Boiler Cycle

An alternate design study was made of a small closed loop one-component steam cycle. The design parameters fixed for this study are as follows:

a. sonic flow at throat

b. throat diameter: 2-3mm

c. nozzle throat static pressure: 35-65 psia

d. saturated steam to exist only at the throat

The system is shown in figure 7. The steam is superheated after leaving the boiler so that condensation occurs only as the steam undergoes a temperature drop as it goes through the converging nozzle leading to the charging region of the generator. A single component charged aerosol stream may be formed in this manner since the ions emitted by the corona field in the charging region serve as condensation centers for the saturated vapor.

The flow requirements for the steam cycle may be calculated from equations (29) and (32):

$$M_* = \delta_* A_* U_* \tag{29}$$

$$U_* = \sqrt{\gamma g RT_*} \tag{32}$$

where δ_* and T_* are obtained from the tables for saturated steam at the nozzle throat pressure specified. The value of the gas constant R for steam is 82.2 ft/lb °R. The inlet pressure may be calculated by the equation

$$P_* = .545\ P_0 \tag{37}$$

The operating conditions for two typical cases are shown in table II.

Table II

OPERATING CONDITIONS FOR CLOSED CYCLE STEAM OPERATION

Nozzle Throat Diameter (mm)	2	3
Throat Area (mm^2)	3.14	7.08
Mach No. at Throat	1	1
Static Pressure at Throat (psia)	34.7	64.7
Total Pressure at Inlet (psia)	63.6	111.9
Mass Flow (kg/min)	0.125	0.5
Boiler Power Requirements (kw)	4.5	17.7
Saturation Temperature at Inlet Pressure (°C)	126	147

III EXPERIMENTAL INVESTIGATION

A. Instrumentation

An instrumented test bench was designed and constructed to measure the temperature, pressure, flow, and electrical parameters required for generator performance evaluation. A schematic of the instrument setup is shown in figure 8. The instrumentation employed are listed in table (A-1) of the appendix. Their functions are explained below:

1. Flow Instrumentation

Three rotameter type flowmeters[4] were used for the measurement of air flow through the generator. The ranges covered were 1.4 - 17.5 scfm, 3.5 - 44.8 scfm, and 8.5 - 100 scfm. Several small liquid rotameters were used to measure aerosol liquid flow.

2. Pressure Instrumentation

A large pressure instrumentation panel [4] was constructed which housed ten pressure gauges of various ranges. These gauges were connected to pressure probes located at various points in the system.

Seven manometers ranging in height from 36 to 110 inches were used to measure differential pressure at various points in the system. These manometers were charged with either mercury or water depending on the pressure range to be covered.

3. Electrical Instrumentation

An electrical instrumentation panel[4] was set up to house the equipment used for measuring the electrical input and output of the generator. This equipment included two electrostatic voltmeters covering the range from 0-50 kilovolts and 0-30 kilovolts, a resistance type kilovoltmeter covering the 0-30 range, and ultra-sensitive micrometers which were used for making current measurements.

4. Temperature Measurements

Temperatures were measured by means of precision laboratory grade thermometers.

Two sections were constructed with adapters to house the pressure probes and thermometers. These sections were inserted in the air line at the inlet and discharge of the generator.

B. Electrojet Studies

1. Reduction of Input Electrical Power Requirements

In the previous studies made of the electrojet method of producing charged aerosol particle streams, the charging current was always greater than the collected current. Means were sought of reducing the current loss so that the output current would equal input current.

This problem was solved by changing the circuitry of the charging system. Previously, the needle was placed at high voltage, while the charging plate was grounded (see figure 9-A). In the revised arrangement shown in figure 9-B, the needle was grounded and the charging plate was placed at high voltage.

In this manner, the input current was reduced to the point at which it was only the value of the leakage current, which was only a small percentage of the output current. The input electrical power requirements to the generator are correspondingly decreased. With proper design, the leakage current may eventually be reduced to a value such that the charging supply will act only as a bias supply.

2. Enclosure of the Conversion Region

In the early electrojet generator tests, the region between the charging plate and the collector was not enclosed. An early electrojet type of unit with an open conversion region is illustrated in figure 10.

Subsequent to the evaluation of this design, a new test generator unit with an enclosed conversion section was designed. This unit is shown in figure 11. Initial tests showed the deposition of a thin conducting film of aerosol liquid upon the walls enclosing the conversion region. This film caused current leakage between the charging plate and the collector. Various shapes were tried for the bore of the enclosing section in order to eliminate film formation. These efforts, however, were all unsuccessful. Efforts were made to break up the film layer by bypassing a portion of the air flow entering the nozzle and injecting it into the conversion region, and by replacing the lucite parts with teflon which has antiwetting properties. This work was also unsuccessful.

Electrojet aerosol particle size was measured to determine whether the existence of large droplets was contributing to the deposition problem. This was done by coating a small glass slide with a light silicone oil and inserting the slide into the conversion region to collect a sample of the aerosol. The slide was examined under a microscope and its size was determined by comparison with a reference scale. A microphotograph was made of the sample. The time between collecting and photographing the droplets was recorded. Then, by determining the coagulation rate from known equations, the mean size could be calculated. The average diameter of the particles just after collection was found to be under one micron. However, there was a wide size distribution and particles as large as five microns in diameter were present in every test made. These large particles were the principle cause of the thin film deposition.

3. Experimental Results with the Electrojet type of EHD Generator

A thorough study[1] of the electrojet type of generator was performed under the previous contract. The maximum output obtained in this study of the electrojet generator was about .30 watt. The performance parameter of this test point is summarized in table III.

Table III

TYPICAL OPERATING CONDITIONS FOR AN ELECTROJET TYPE OF EHD GENERATOR

Nozzle Throat Diameter (mm)	3
Throat Area (mm^2)	7.08
Total Pressure at Inlet (psia)	114.7
Input Voltage (kv)	3.0
Input Current (microamperes)	8.0
Input Power (watts)	.024
Output Voltage (kv)	12.5
Output Current (microamperes)	24
Output Power (watts)	.300
Net Electrical Power Output (watts)	.276
Power Density ($watts/m^2$)	39,000

C. Condensation Aerosol Unit Studies

1. Production of Charged Aerosol Particles

In order to obtain aerosol particles smaller than those produced by means of the electrojet method, aerosol particles were produced by condensation of the vapor in the air stream. The liquid for the aerosol was injected into the air stream upstream of the generator by means of a small atomizer connected into the air line. An electrojet type of unit, with its liquid feed system disconnected, and the hollow needle replaced by a tungsten wire, was used to provide the corona discharge for the new condensation aerosol generator. The unit tested initially is shown in figure 12.

Operation with this unit also resulted in the formation of a thin conducting film after a few minutes of operation. Eventually an excess of liquid was being injected into the air stream, and, as a result, a small fine metering valve was installed between the outlet of the atomizer and the injection point in the air stream. Even with the valve completely closed off (no liquid injection), the thin conducting film was formed. Apparently the water vapor present in the ambient air provided a sufficient quantity of condensed aerosol.

A large silica gel dryer was placed in the air line upstream of the generator to dry the compressed air. Twenty pounds of silica gel were sufficient to permit operation of the generator for several hours without interference of film formation.

Attempts were made to measure the size of the particles produced by the condensation aerosol process. The particles were too small to be measured using the sampling process described for the electrojet generator. Light scattering techniques were also ineffectual since the particles were apparently less than 0.2 micron in diameter which is below the size limit of this method. Evidently, the particles produced by the condensation technique were less than one fifteenth of the diameter of those produced by the electrojet method. Evidence that particles were formed was obtained by noting that when the silica gel was first inserted into the air line, operation of the generator was not possible unless some liquid was injected to the line.

2. Electrical Performance

An experimental study of the effect of generator inlet pressure upon the electrical performance of a condensation aerosol type of generator was made. A unit similar to that in figure 12 with a 3mm diameter nozzle throat was used. Ethyl alcohol was injected into the air stream after the water vapor in the air was removed by the silica gel filter. The results of the tests are presented graphically in figures 13 through 15.

A plot of input voltage vs output voltage is shown in figure 13. The output voltage is shown to increase with input voltage and operating pressure level.

The variation of input and output current with inlet pressure for two values of input voltage are shown in figure 14. The input current is seen to decrease rapidly with increasing pressure. Below 105 psia for 4 kilovolts input voltage, the input current is always greater than the output current. It can be seen from this graph that at some critical value of pressure, dependent upon the input voltage, the input current decreases below the output current.

Plots of input electrical power and output electrical power vs pressure are shown in figure 15. From the curves, it is easily seen that the input power requirements decline rapidly with increasing pressure while the output power increases rapidly with increasing inlet generator pressure in the range under consideration (60 to 110 psig). For an input voltage of 4 kilovolts,

a net power gain is not obtained until the inlet static pressure is above 73 psig.

3. Aerodynamic Behavior of the Generator

A fully instrumented condensation aerosol EHD generator was constructed to study the aerodynamic behavior of the generator. The instrumented unit is shown schematically in figure 16.

Total pressure probes, as well as static pressure taps, were placed in the inlet and the collector sections of the generator. Instrumentation housing sections, containing total pressures probes and thermometers, were inserted upstream of the fluid injection section, and downstream of the collector. Pressure gauges were used to measure the static and total pressures downstream and upstream of the generator. The total pressure change between the generator inlet and the collector was measured by mercury manometers. The flow through the unit was varied by a gate valve placed downstream of the second instrumentation housing section. Air flow through the unit was measured by three rotameters inserted upstream of the generator.

Mach number was determined by flow rate, total pressure, static pressure, and temperature measurements at several points throughout the system. A plot of Mach number at the entrance to the charging plate, vs the normalized total pressure drop between the generator inlet and the collector section is shown in figure 17. Station (3) refers to the collector while station (2) refers to the nozzle inlet. As shown in figure 17, Mach

number of the charging plate inlet remains constant as the normalized pressure drop increases above .18. This is the point at which choking occurs at the exit of the plate.

4. The Effect of Mach Number Upon the Electrical Performance of the Generator

A thorough study of the effect of Mach number upon the electrical performance was made. Whereas in previous generator performance studies only inlet pressure was varied, downstream pressure was varied in this test by means of a gate valve.

The condensation aerosol unit used in the tests described previously was employed for this study. The inlet pressure was kept fixed at 100 psig. The value of the input voltage was set just below the incipient breakdown voltage for the corona point-charging plate electrode configuration.

The electrical output power as a function of the normalized total pressure drop across the generator is shown in figure 18. The maximum electrical output power as seen from the curve is about 2.25 watts. This occurred for a normalized total pressure drop of about .18 which corresponds to the nozzle throat just becoming choked.

The conversion efficiency may now be calculated from equation (15):

$$\eta_c = (P_{out} - P_{in})/U_n A d(\Delta P) \qquad (15)$$

The denominator, which is the energy change of the gas stream due to the electrical power extraction, is plotted in

figure 18 as the available power. The conversion efficiency as a function of nozzle inlet Mach number and normalized pressure drop is shown in figure 19.

It is apparent from figure 19 that the conversion efficiency reaches a maximum value of about 82 percent as the nozzle throat Mach number approaches one. The conversion efficiency begins to drop off as the region downstream of the nozzle becomes supersonic. A maximum power output of 2.25 watts was obtained with a 3mm diameter nozzle throat. This corresponds to a power density of 318,000 watts/m^2 which is almost an order of magnitude greater than the power density of about 39,000 watts/m^2 obtained with the electrojet generator.

The performance parameters for the maximum power output test point are summarized in table IV.

Table IV

TYPICAL OPERATING CONDITIONS FOR A CONDENSATION AEROSOL TYPE OF EHD GENERATOR

Nozzle Throat Diameter (mm)	3
Throat Area (mm^2)	7.08
Total Pressure at Inlet (psia)	114.7
Total Pressure at Collector (psia)	74.7
Input Voltage (kv)	7.54
Input Current (microamperes)	6.0

Table IV (Cont'd) TYPICAL OPERATING CONDITIONS FOR A CONDENSATION AEROSOL TYPE OF EHD GENERATOR	
Input Power (watts)	.045
Output Voltage (kv)	35.9
Output Current (microamperes)	62
Output Power (watts)	2.25
Net Electrical Power Output (watts)	2.18
Power Density (watts/m^2)	310,000

5. Series Operation of Condensation Aerosol Type Generator

Two condensation aerosol generators were operated in series to test the feasibility of series operation. The system is shown schematically in figure 20. As shown in figure 20, a portion of the flow through the first unit had to be diverted from the second unit. This had to be done since the flow requirement for sonic operation is much greater for the first generator due to its higher operating pressure level. In future designs the flow which will be bled off from the first unit will pass through a second unit in parallel with the second generator arranged in series. Fluid was injected only upstream of the first unit. After the aerosol particles deposited their charges in the collector of the first unit, they re-evaporated in the air stream and were available for condensation of the second unit. A capacitor placed across a portion of the load resistance of the first unit provided the charging voltage for the second unit.

The output of the second unit was somewhat smaller than the first due to the decreased flow and inlet pressure level. Using the output voltage of the first unit as a ground for the second unit, a total output voltage of about 50 kilovolts was obtained. No further tests with the series units were performed since the prime emphasis must be given to optimizing the first generator stage before generator series staging can be thoroughly evaluated. The success of the two series units makes possible maximum utilization of the available gas stream power.

D. Closed Cycle Air Compressor System

A one-horsepower refrigeration unit was purchased to be used as a test vehicle for a compressed air closed cycle system. The unit as purchased is shown in figure 21. Appropriate valves and pressure gauges were installed in the system to modify it for our purposes. A section of clear lucite in the shape of a small nozzle was placed in the system to observe the flow through it. An orifice plate type flow meter was used to measure the flow.

Upon initial testing of the system, it was found that oil from the compressor was contaminating the air stream. Several oil separators had to be installed to remove the oil.

The surge tank in existence on the system did not damp out the pressure oscillations caused by the compressor. A larger surge tank used in place of the smaller one, effectively dampened out the pressure oscillations.

A bypass line was inserted to allow some of the warm air from the compressor to bypass the cooler and enable variation of the air temperature entering the generator. The system as it finally evolved is shown in figure 22.

The high pressure drops encountered throughout the system resulted in a very low inlet pressure to the lucite nozzle simulating the generator. Considering the pressure losses and the low flow capacity of the system, the output electrical power would be too low to serve as an experimental unit. For these reasons, the project of building a small closed loop was abandoned for the present.

A design study of a larger closed loop was made and the results are presented in table I of this report.

IV CONCLUSIONS

The development of a charged aerosol electric generator has progressed from a unit which demonstrated the EHD conversion concept, to an evaluated system capable of assembly into a complete thermodynamic cycle. In order to reach this stage, many instrumentation, technical, and design problems had to be investigated and solved.

A. Enclosing the Conversion Section

Previously developed electrojet techniques produced a uniform sized aerosol. However, the particle size increased rapidly after formation and, as a result, a wide range of particle size distribution was obtained with a measured mean radius of approximately 5 microns. These large droplets condensed on the walls of an enclosed conversion section and produced a leakage path between the charging plate and the high voltage collector. Several unsuccessful trials were made to prevent the formation of this leakage path by using different wall materials. It was finally decided to abandon the electrojet method of producing the aerosol in favor of forming the water particles by condensation of the water vapor in a saturated air mixture. Condensation was induced by expansion of the air stream in a convergent nozzle and the condensate particles were formed and charged in a corona field located at the nozzle throat. This condensation technique allowed enclosure of the conversion region and increased the output

current by more than 300%. However, this technique required sonic or near sonic conditions at the nozzle throat in order to obtain appreciable power output levels.

B. Input Current to the Generator

The input current requirements from an external supply were minimized by modifying the circuitry. This was accomplished by recirculating the output current from the ground end of the load resistor. As a result the external input current was reduced to the value of the leakage current through the charging plate. This amounted to a few per cent of the output current.

C. Theoretical Considerations

A theoretical study of the thermodynamic variables associated with the mechanics of the aerosol was made to aid in guiding our experimental efforts. The two main objectives of the analysis were as follows:

1. To properly define the efficiency of each phase involved in the conversion process. This was required in order to relate open cycle measured values to the overall efficiency of the generator. The result was to adopt the following definitions:

$$\text{Ideal Cycle Efficiency } \eta_i = \frac{\text{Isentropic Generator Work}}{\text{Actual Pump Work + Heat Added}}$$

$$\text{Generator Efficiency } \eta_g = \frac{\text{Generator Output}}{\text{Isentropic Generator Work}}$$

$$\text{Overall Efficiency } \eta_{ov} = \eta_i \eta_g = \frac{\text{Generator Output}}{\text{Actual Pump Work + Heat Added}}$$

Using these definitions (see figure 3), it was concluded that for a fixed system pressure ratio (P_2/P_3), η_1 decreased with increasing temperature ratio (T_2/T_{31}).

For small conversion sections and single stage operation, the generator's efficiency, η_g, can be closely approximated by incompressible flow analysis:

$$\eta_g = \frac{\text{Power Output}}{\text{Flow times Pressure drop}}$$

Pressure drop is the sum of two terms: a frictional pressure drop, mainly dependent on nozzle geometry and gas velocity; and an electrodynamic pressure drop which is brought about by the conversion of flow energy into electrical energy. The electrodynamic pressure drop was used to define a conversion efficiency, η_c. Its measurement determines the efficiency of kinetic to electrical energy conversion disregarding frictional losses due to wall friction, or discontinuities on the nozzle surface.

2. To study the effects of nozzle shape on generator's performance. This study resulted in specifying a multislot airfoil nozzle as the most desirable geometry to minimize frictional losses. The airfoil design, however, can only prove to be effective for large cross-sectional areas.

D. Instrumentation

A fully instrumented test stand was built for the measurement of gas flow, velocity, pressure, and temperature. The instrumentation for measuring operating pressure and pressure

drop across the generator was arranged such that the pressure drop due to wall friction and that due to electrodynamic effects could be determined separately. The conversion efficiency, η_c, was measured at 83% for an input pressure level of 120 psig and a 3mm nozzle throat. The maximum electrical output power for this nozzle was 2.25 watts. The generator efficiency, η_g, was only about 0.1% due to high wall frictional losses, and the presence of a flow discontinuity on the nozzle's wall at the entrance of the conversion section.

E. Generator Staging

Experimentally, it was demonstrated that staging of two generators was possible and in fact, inherent in the operation of a generator using the condensation technique. The second stage generator did not require either an external voltage supply for ionization, or a liquid supply to produce the aerosol's droplets.

F. Closed Cycle Studies

Some analysis and preliminary experimentation were conducted in order to gain familiarity with the problems associated with enclosing the generator in a thermodynamic cycle. The results were mainly helpful in estimating component sizes and are by no means conclusive.

V FUTURE WORK

Future work will be directed towards the construction of a closed cycle, high voltage, high power density system. Each component will be individually investigated in order to evaluate their design parameters. The cycle will operate at temperatures higher than room temperature and the experimentation will encompass studies with thermal energy as the input energy to the system. Before this work is conducted, however, the generator requires some further open cycle experimentation to increase its output and efficiency. Once this is done, the type of cycle and system components can be more precisely specified. An experimental airfoil type unit will be tested and the nozzle shape will be optimized to eliminate surface discontinuities. The problem of current leakage along the walls will be investigated. It is anticipated that by constructing a collector which does not contact the nozzle wall, current leakage will be eliminated leaving electric breakdown as the only limitation to output voltage and power.

Electric breakdown in a charged aerosol is, for the most part, an uninvestigated phenomena; experimental and theoretical studies must be conducted, particularly with regard to charge density limitations and thermodynamic effects.

The design of a closed cycle will be based on the use of a condensible fluid as the carrier gas. This fluid will be evaporated before the generator and condensed afterwards so

that only a small liquid pump is required to bring the liquid back to the operating pressure level of the boiler. Initial testing will be performed using steam because of its simplicity in producing and handling, and because of the large amount of data available in the literature on this material. Once we are familiar with the design of a closed cycle EHD system using a condensible carrier gas, the use of more exotic materials will be investigated for improving system performance.

VI REFERENCES

1. Final Report, "The Conversion of Heat to Electrical Power by Means of a Charged Aerosol," Contract NOw 60-0831-c
2. Monthly Progress Letter No. 6, The Conversion of Heat to Electrical Power by Means of a Charged Aerosol," Contract NOw 62-0644-c
3. Monthly Progress Letter No. 4, "The Conversion of Heat to Electrical Power by Means of a Charged Aerosol." Contract NOw 62-0644-c, Enclosure #1
4. Monthly Progress Letter No. 5, "The Conversion of Heat to Electrical Power by Means of a Charged Aerosol," Contract NOw 62-0644-c, figures (4), (6), and (7)

Table A-I

INSTRUMENTATION EQUIPMENT

Item	No.	Instrument	Manufacturer	Type	Scale Range	Subdivision
1	2	Manometer	Uehling Inst. Co.	U Tube with 2 Over Pressure Traps No. 80M	40"-0-40"	0.1"
2	2	Manometer	Uehling Inst. Co.	U Tube with 2 Over Pressure Traps No. 50M	25"-0-25"	0.1"
3	1	Manometer	Uehling Inst. Co.	U Tube with 2 Over Pressure Traps No. 110M	55"-0-55"	0.1"
4	2	Manometer	King Gage Co.	U Tube	18"-0-18"	0.1"
5	4	Pressure Gauge	Helicoid Gage Co.	4 1/2" Type No. 410 Alcalloy Case	0-200 PSIG	2 lbs
6	11	Pressure Gauge	Helicoid Gage Co.	4 1/2" Type No. 410 Alcalloy Case	0-100 PSIG	1 lb
7	3	Pressure Gauge	Helicoid Gage Co.	3 1/2" Type 410 Alcalloy Case	0-200 PSIG	2 lbs

Table A-I (Cont'd)

INSTRUMENTATION EQUIPMENT

Item	No.	Instrument	Manufacturer	Type	Scale Range	Subdivision
8	1	Flowmeter Air Flow	Fisher-Porter	Rotameter No. 10A 2735CA	% Scale 100 scfm max.	1%
9	1	Flowmeter Air Flow	Fisher-Porter	Rotameter No. 10A 2735CA	% Scale 17.5 scfm max	1%
10	1	Flowmeter	Fisher-Porter	Rotameter No. 10A 2735CA	% Scale 44.8 scfm max	1%
11	1	Flowmeter	Fisher-Porter	Rotameter No. 25519502	Δ Further Details on Table A-II	
12	1	Microammeter	Simpson Electric	No. 1329c	0-200μa	5 micro-amps
13	2	Microammeter	Simpson Electric	No. 1329c	0-100μa	2 micro-amps
14	3	Ultra Sensitive Micro-ammeters	R.C.A.	WV-84B	0-.01 μ 0-.1 μa 0- 1 μa 0-10 μa 0-100 μa 0-1000 μa	.001 μa .001 μa .01 μa .10 μa 1.0 μa 10.0 μa
15	1	Electrostatic Voltmeter	Sensitive Research Instruments	Model ESH	0-10 KV 0-50 KV	0.1 KV 0.5 KV

Table A-I (Cont'd)

INSTRUMENTATION EQUIPMENT

Item	No.	Instrument	Manufacturer	Type	Scale Range	Subdivision
16	1	Electrostatic Voltmeter	Sensitive Research Instruments	Model ESH	0-5 KV 0-10 KV 0-20 KV	
17	3	Thermometer	Ertco-Palo Labs	No. 48045	0-51°C	0.1°

Table A-II

LIQUID FLOW METERS

Tube Number	Division	Flow - cc/min.	
		S.S. 316 Float	Sapphire Float
FP1/16-20-G-5	20	10.3 max.	4.82
FP1/8-25-G-5	25	107.0 max.	64.50

DWG # 111-7-1

FIGURE 1

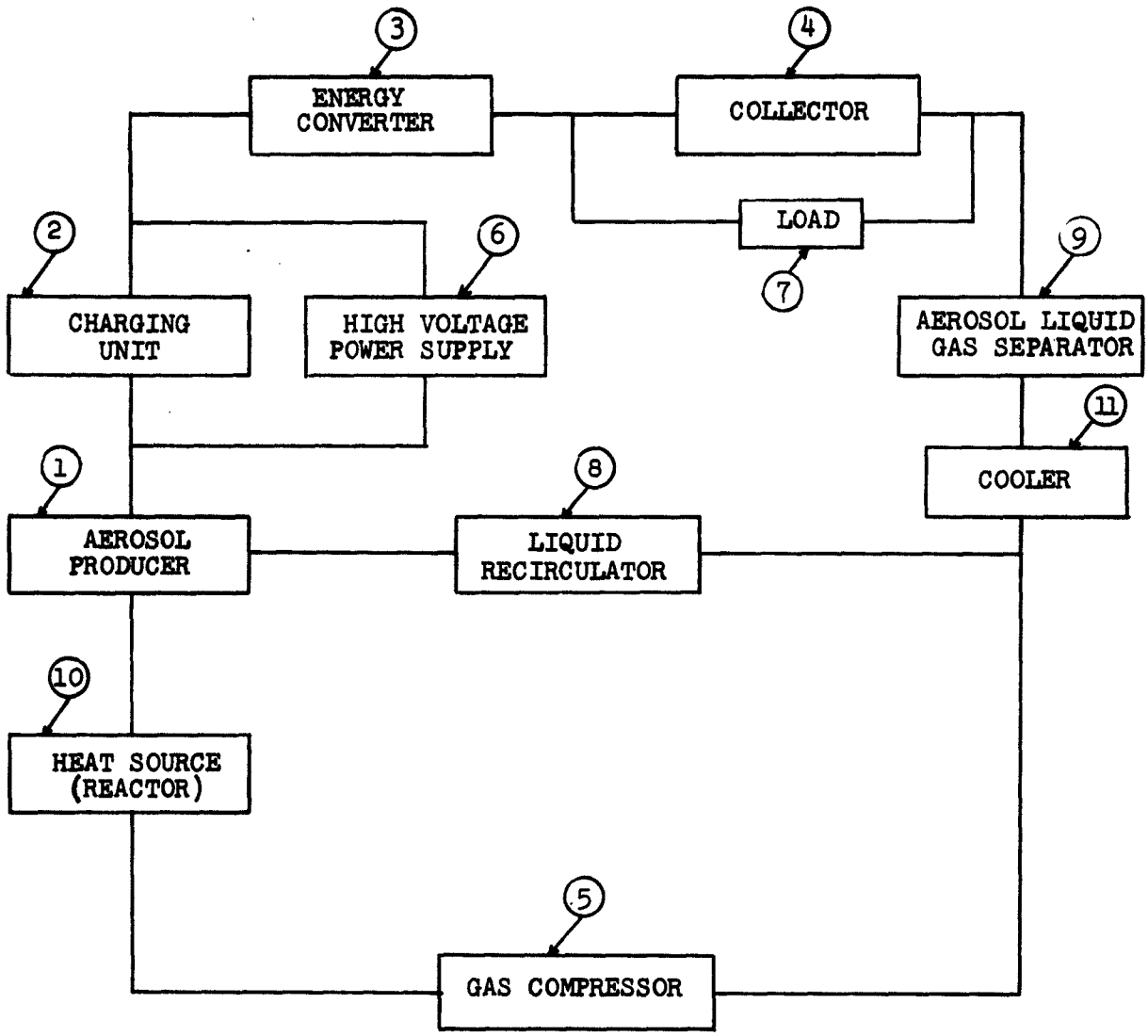

CLOSED LOOP CYCLE SCHEMATIC

DWG # 111-7-2

FIGURE 2

TEMPERATURE ENTROPY DIAGRAM

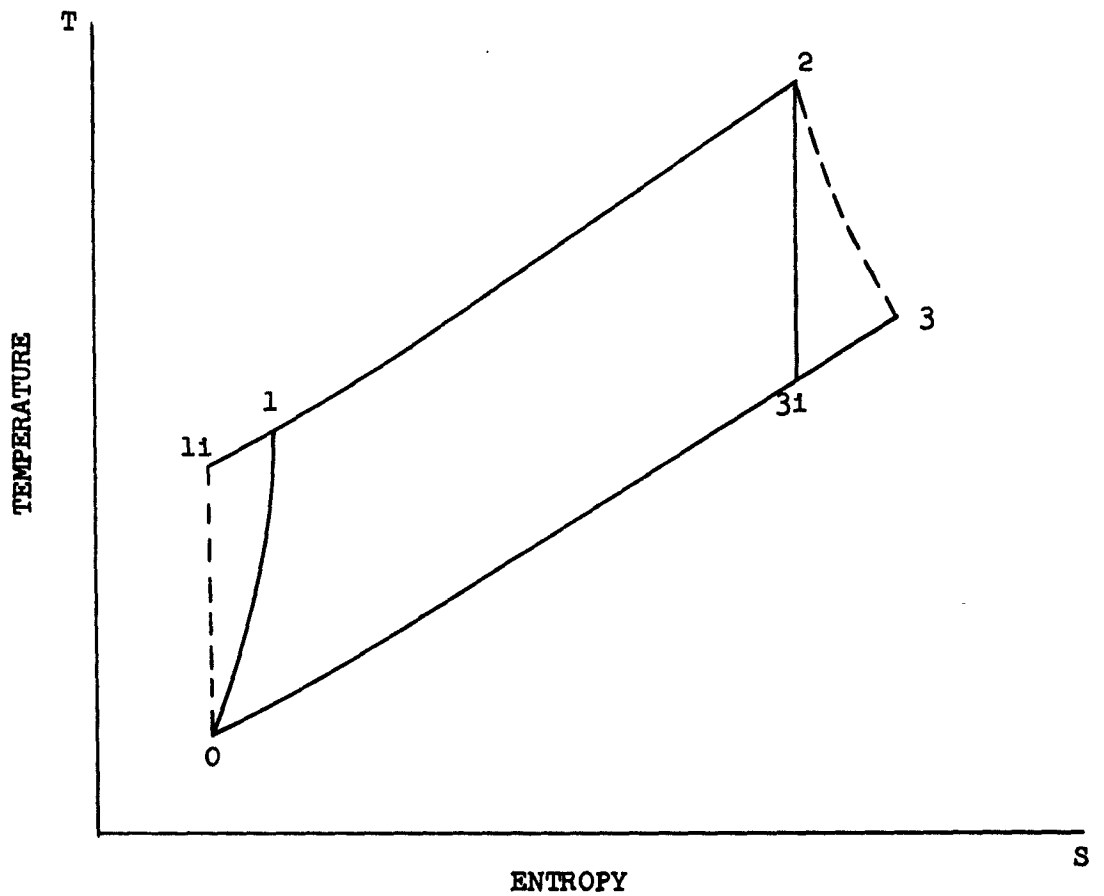

IDEAL CYCLE EFFICIENCY Vs TEMPERATURE
RATIO FOR DIFFERENT PRESSURE RATIOS

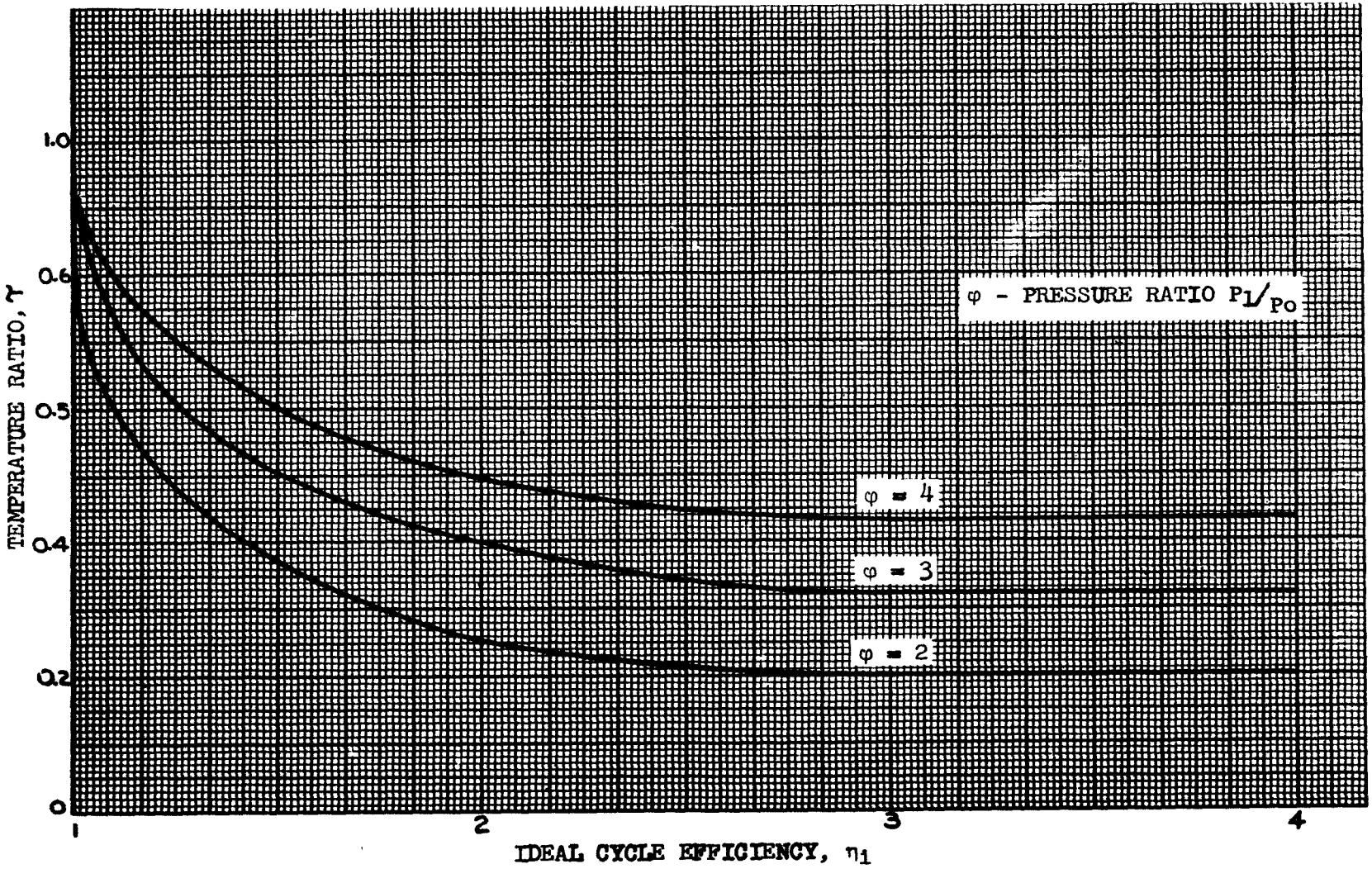

DWG # 111-7-3

FIGURE 3

DWG # 111-7-4

FIGURE 4

AEROSOL ELECTROJET DROPLET FORMATION

STAGE 1 (IDEALIZED). DROPLET SHOWN IN FIRST STAGE AS IT STARTS TO FORM INDICATING SURFACE CHARGING IN APPLIED ELECTRIC FIELD

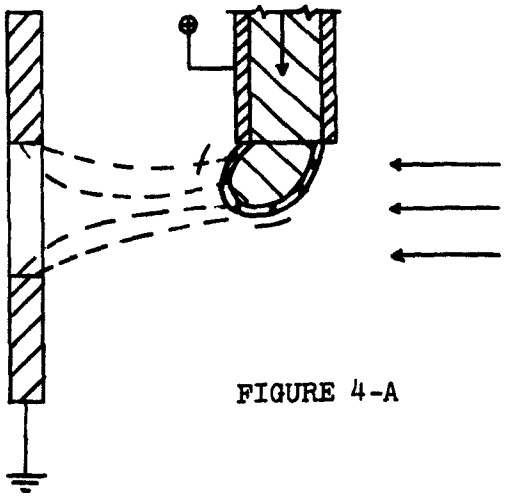

FIGURE 4-A

STAGE 2 (IDEALIZED). DROPLET SHOWN IN SECOND STAGE AS IT INCREASES IN SIZE AND IS JUST ABOUT TORN AWAY FROM THE MAIN BODY OF THE LIQUID, SURFACE CHARGE IS MAINTAINED

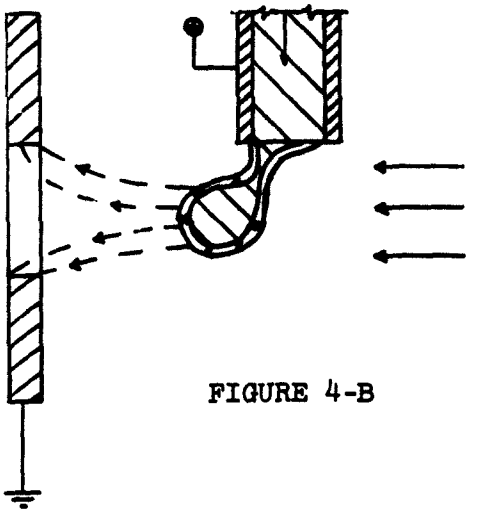

FIGURE 4-B

STAGE 3 (IDEALIZED). DROPLET SHOWN FULLY DETACHED, CHARGED AND CARRIED BY AIR STREAM

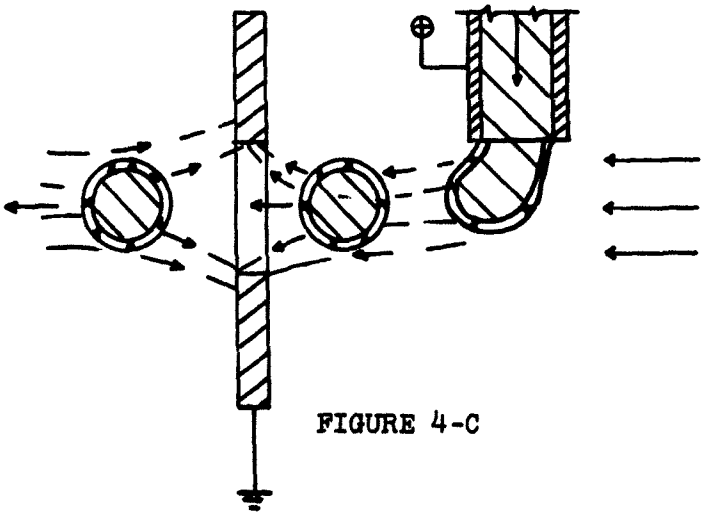

FIGURE 4-C

STAGE 4 (IDEALIZED). SHOWING SIMULTANEOUS MULTIPLE CHARGED DROPLET FORMATION

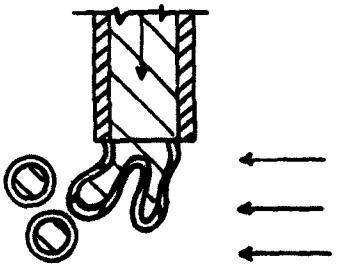

FIGURE 4-D

DWG # 111-7-5

FIGURE 5

GAS PRESSURE VERSUS PARTICLE RADIUS FOR SEVERAL VALUES OF ELECTRONIC CHARGE PER PARTICLE, N

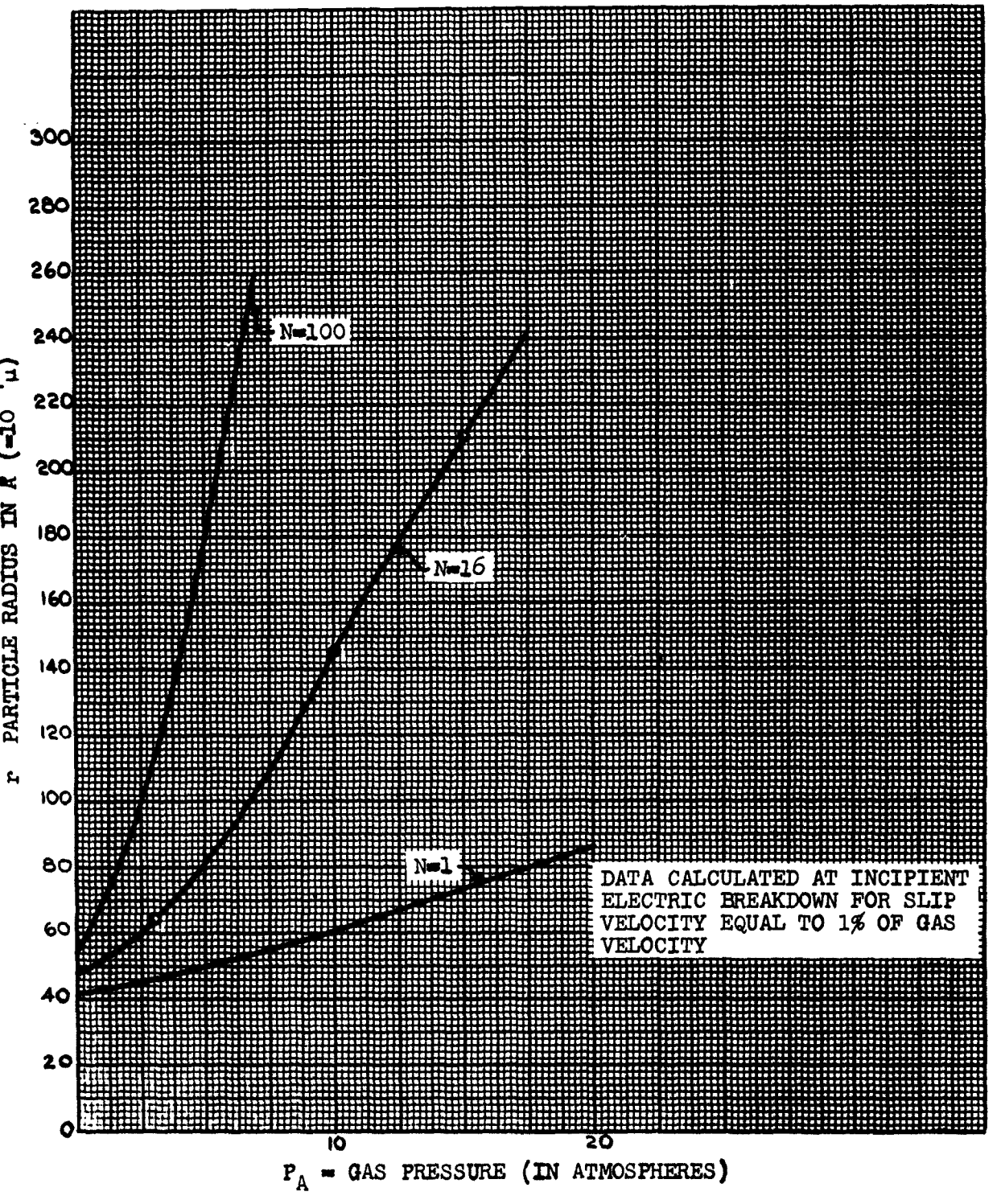

DWG # 111-7-6

FIGURE 6

AIR COMPRESSOR LOOP

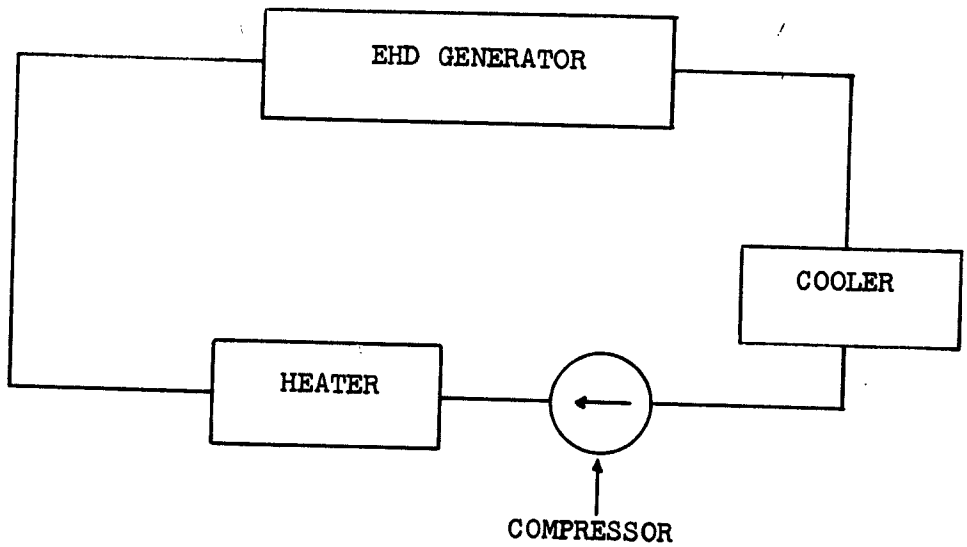

SCHEMATIC OF A TYPICAL VAPOR CYCLE SYSTEM

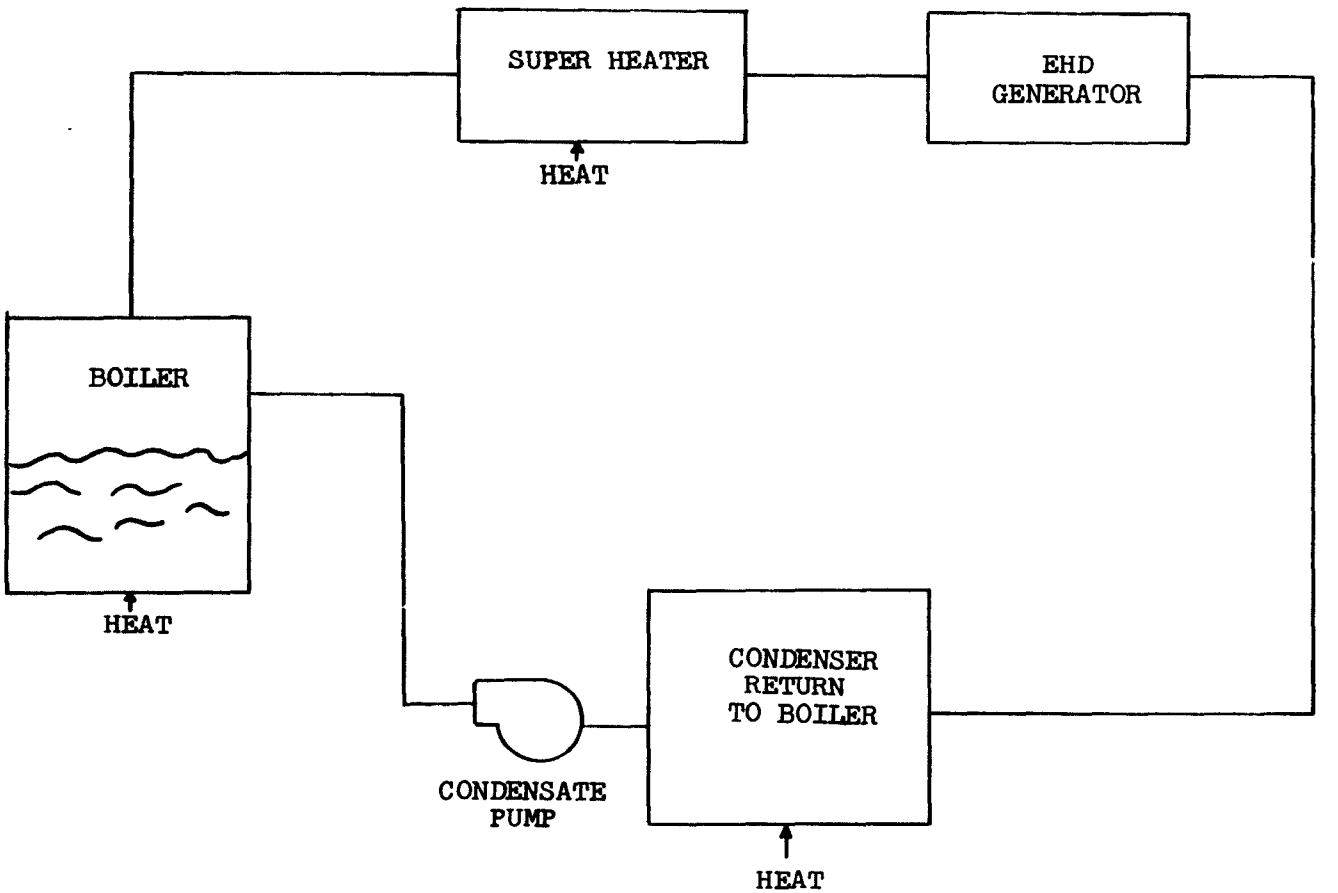

DWG # 111-7-7

FIGURE 7

DWG # 111-7-8

FIGURE 8

SCHEMATIC OF INSTRUMENTED CONVERTER TEST UNIT

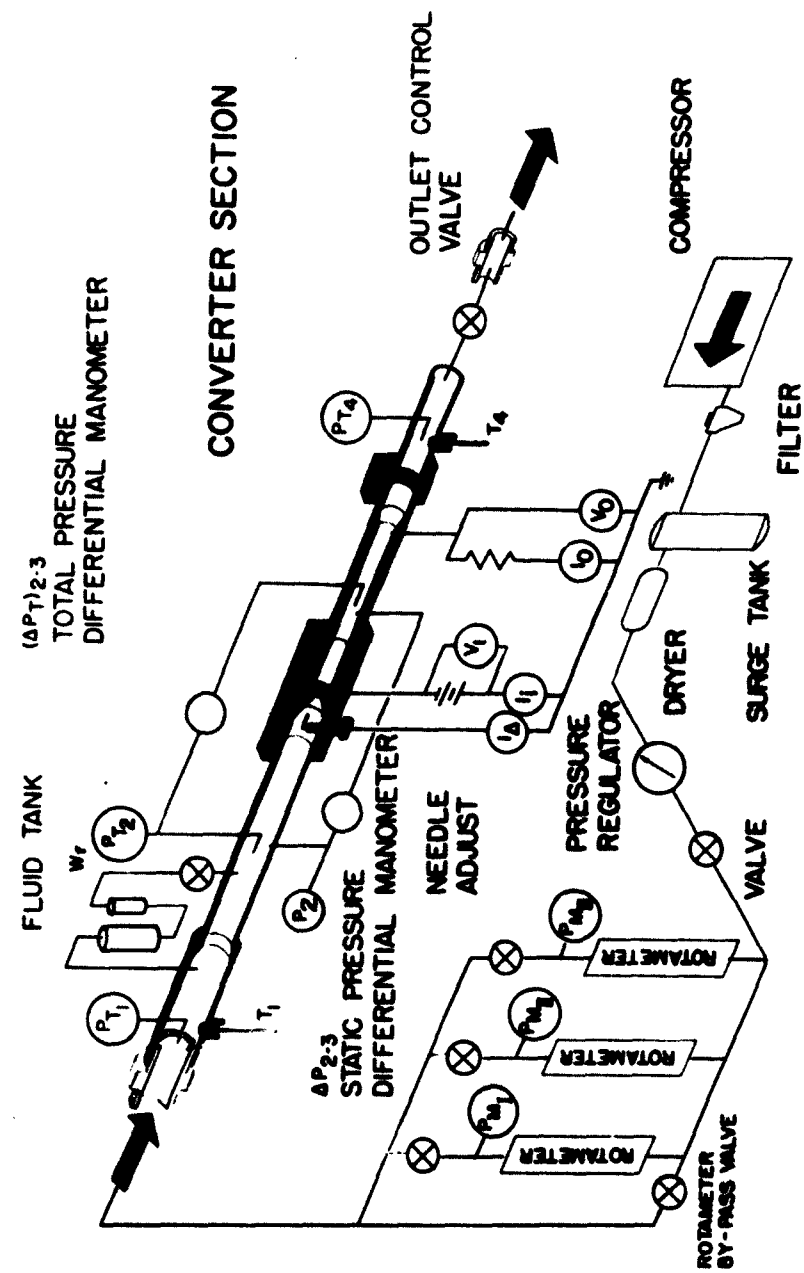

DWG # 111-7-9 FIGURE 9

GENERATOR CIRCUITRY FOR THE CORONA DISCHARGE

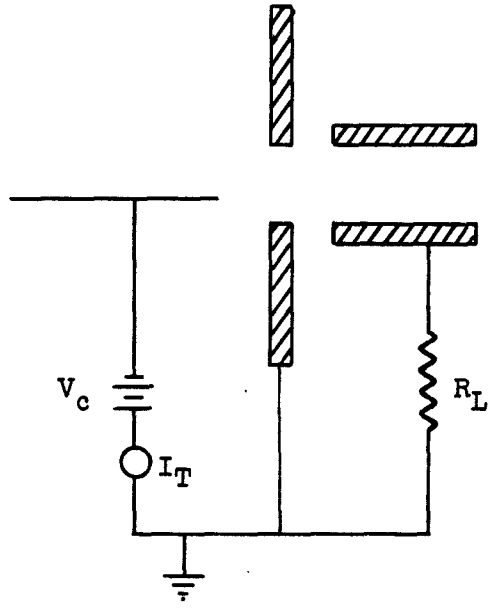

FIGURE 9-A. ORIGINAL CHARGING CIRCUIT

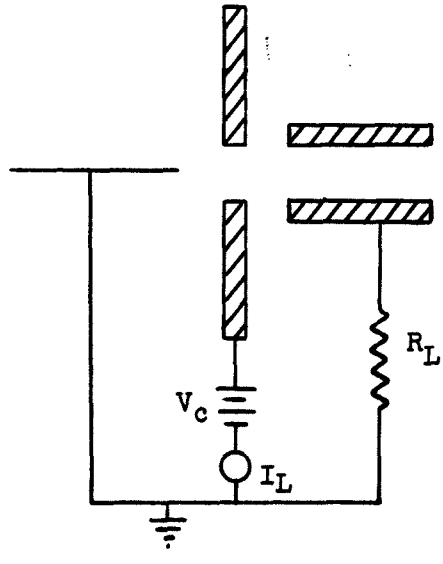

FIGURE 9-B. MODIFIED CHARGING CIRCUIT

DWG # 111-7-10

FIGURE 10

ELECTROJET TEST GENERATOR
OPEN CONVERSION SPACE

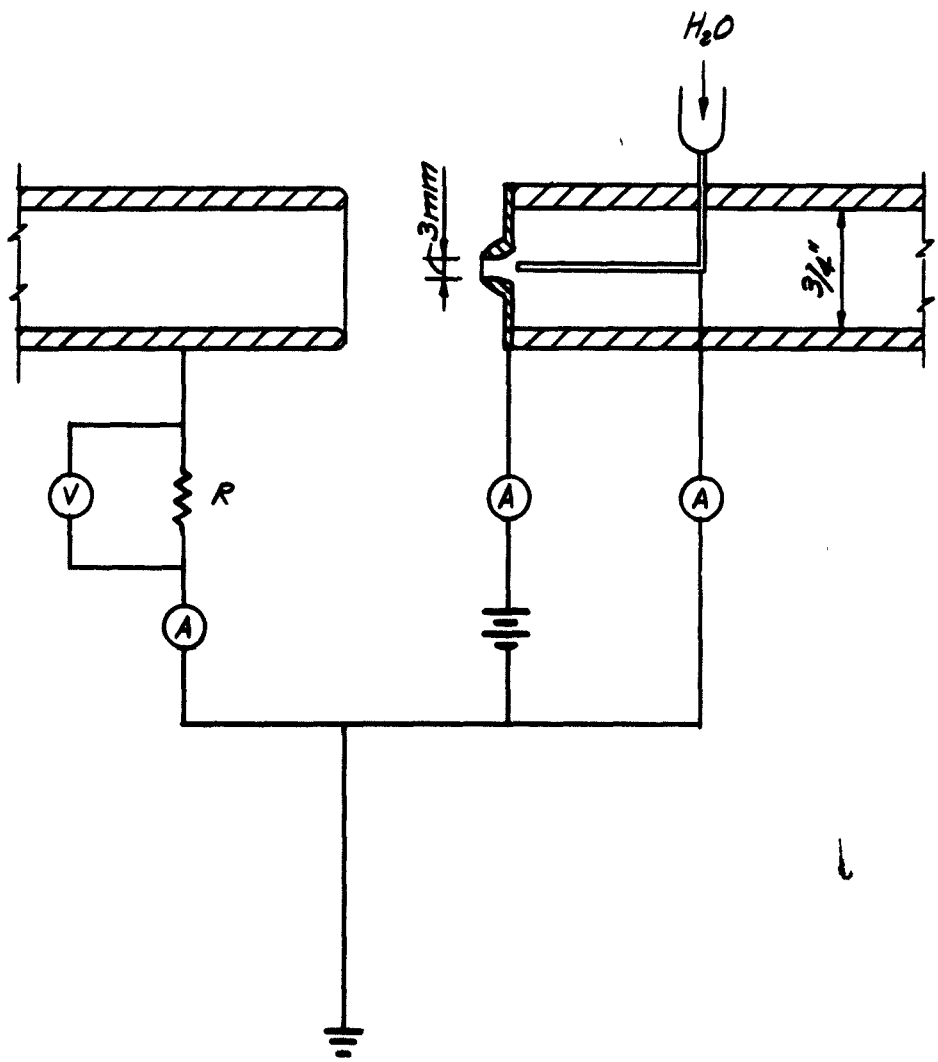

DWG # 111-7-11

ELECTROJET TEST GENERATOR
ENCLOSED CONVERSION SPACE

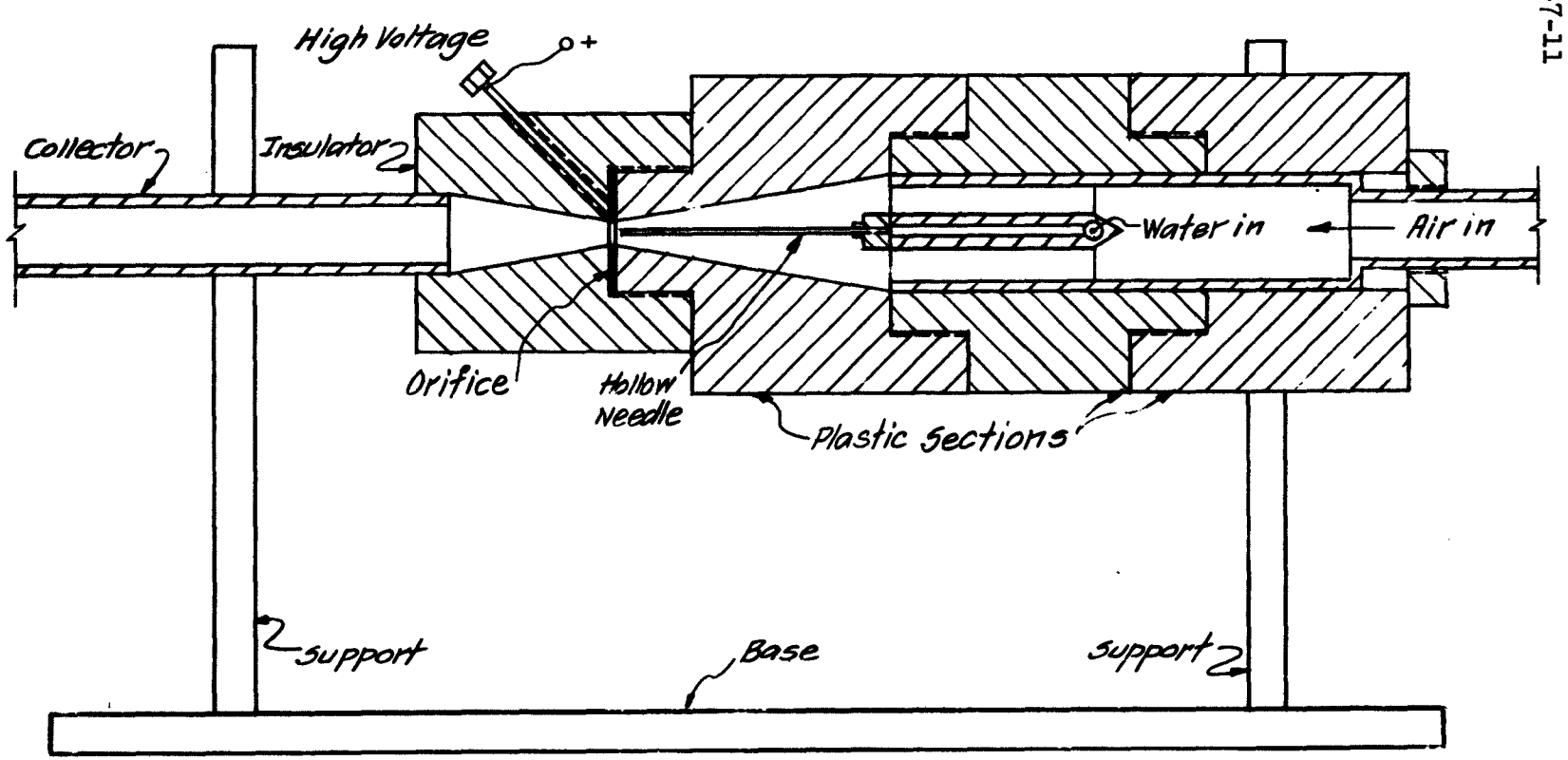

FIGURE 11

TEST GENERATOR USING CONDENSATION TYPE AEROSOL

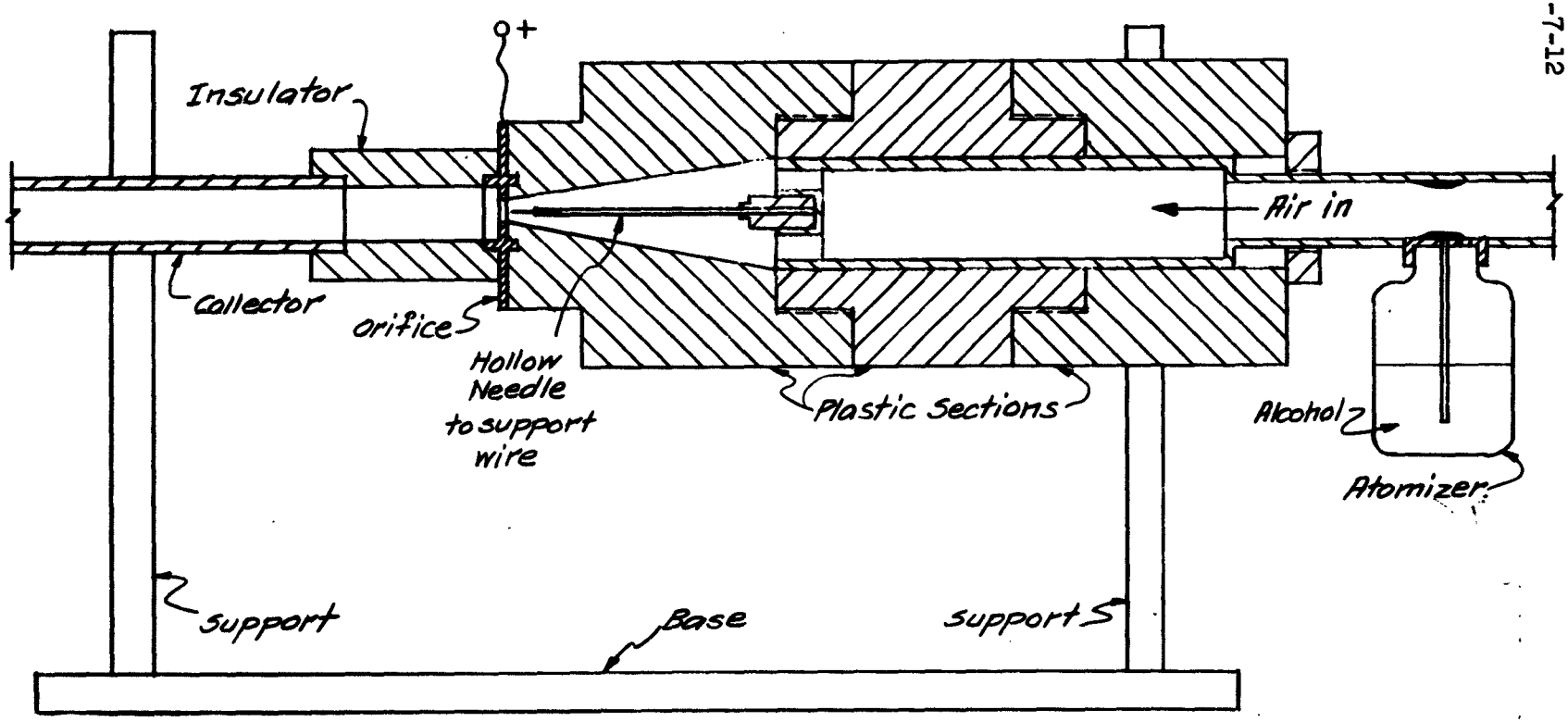

DWG # 111-7-12

FIGURE 12

DWG # 111-7-13

FIGURE 13

OUTPUT VOLTAGE VERSUS INPUT VOLTAGE
AT VARIOUS ABSOLUTE PRESSURES

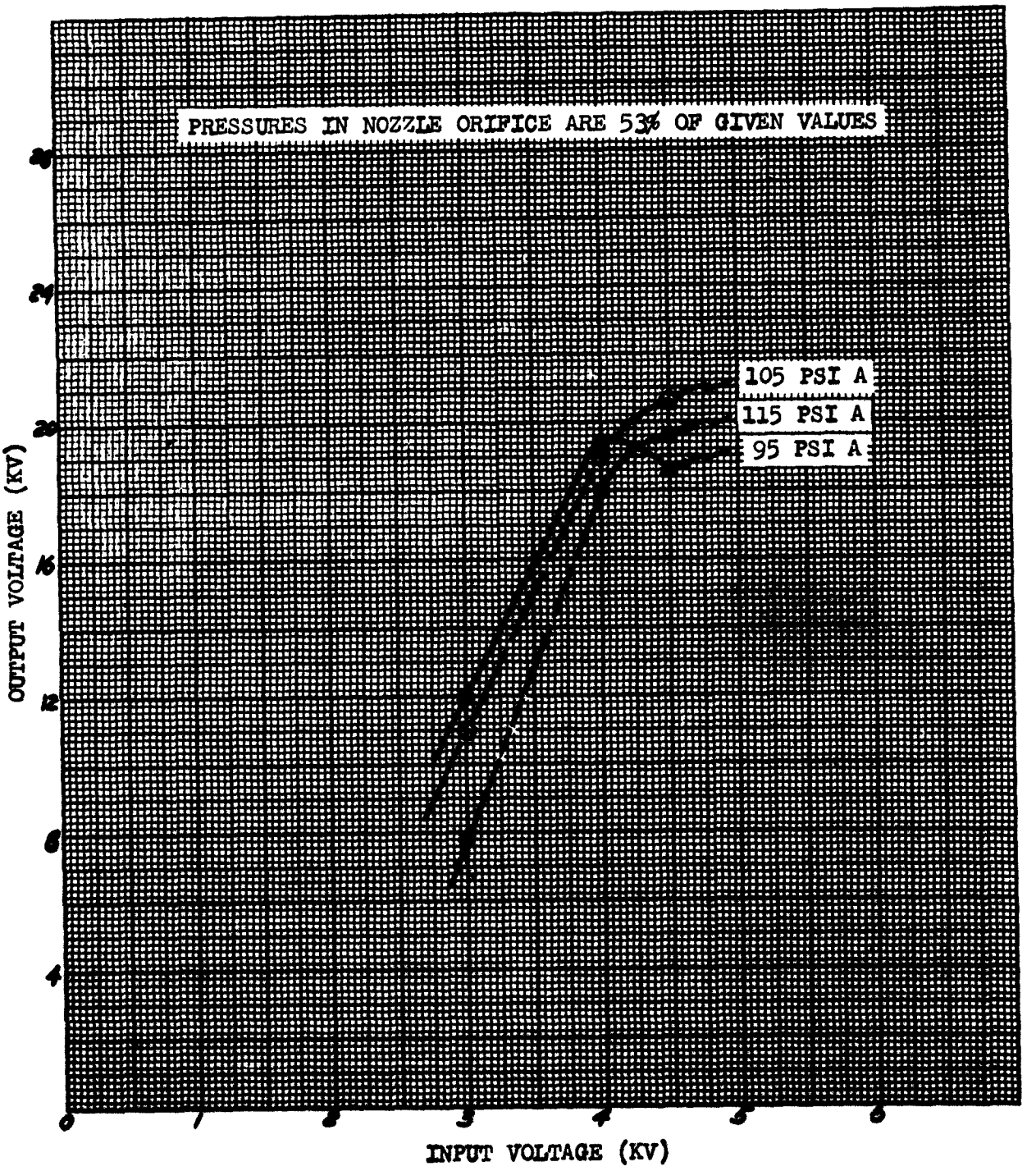

DWG # 111-7-14

FIGURE 14

OUTPUT CURRENT AND INPUT CURRENT VERSUS
INLET ABSOLUTE PRESSURE FOR TWO DIFFERENT
VALUES OF CHARGE PLATE VOLTAGE

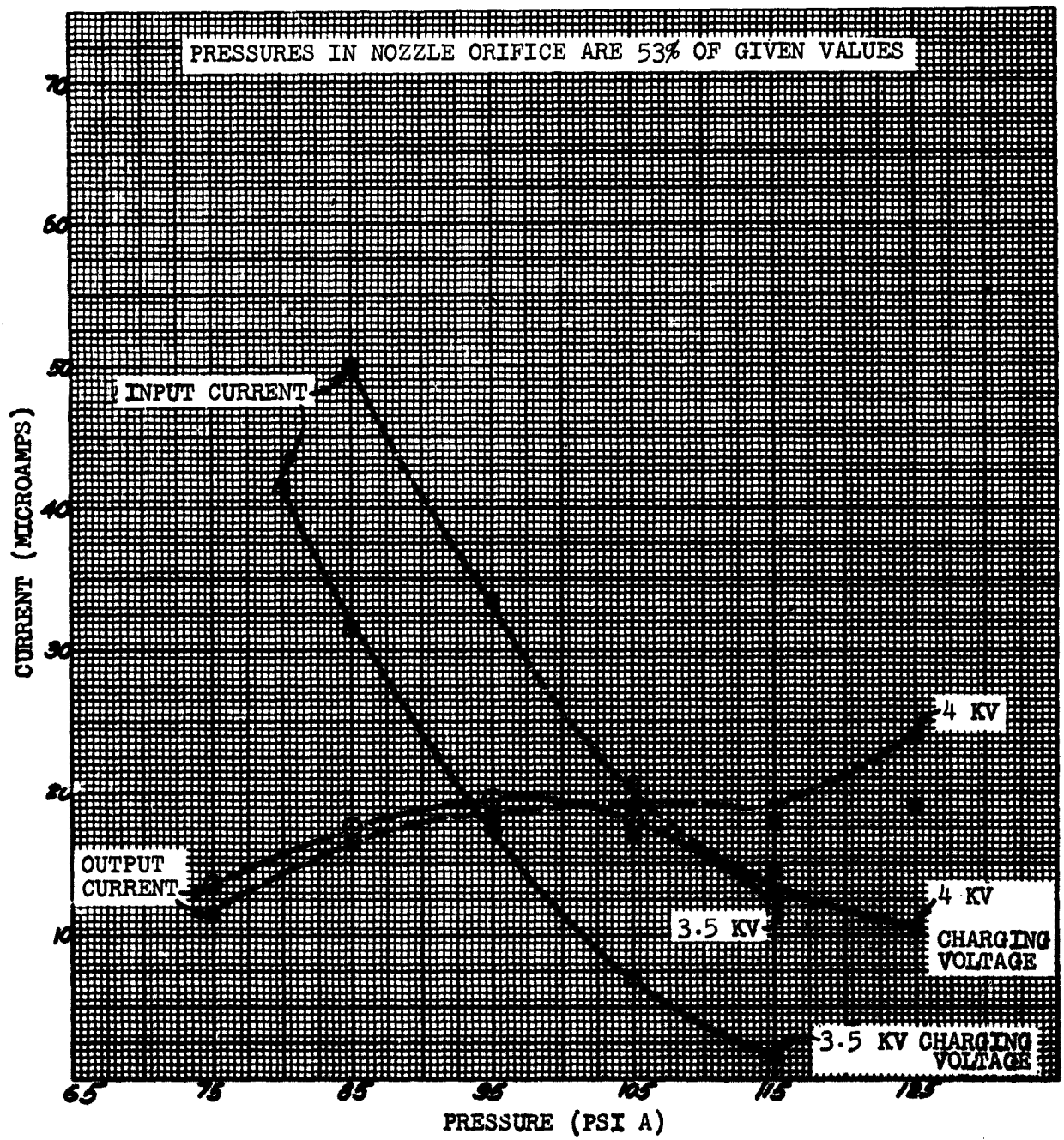

DWG # 111-7-15

FIGURE 15

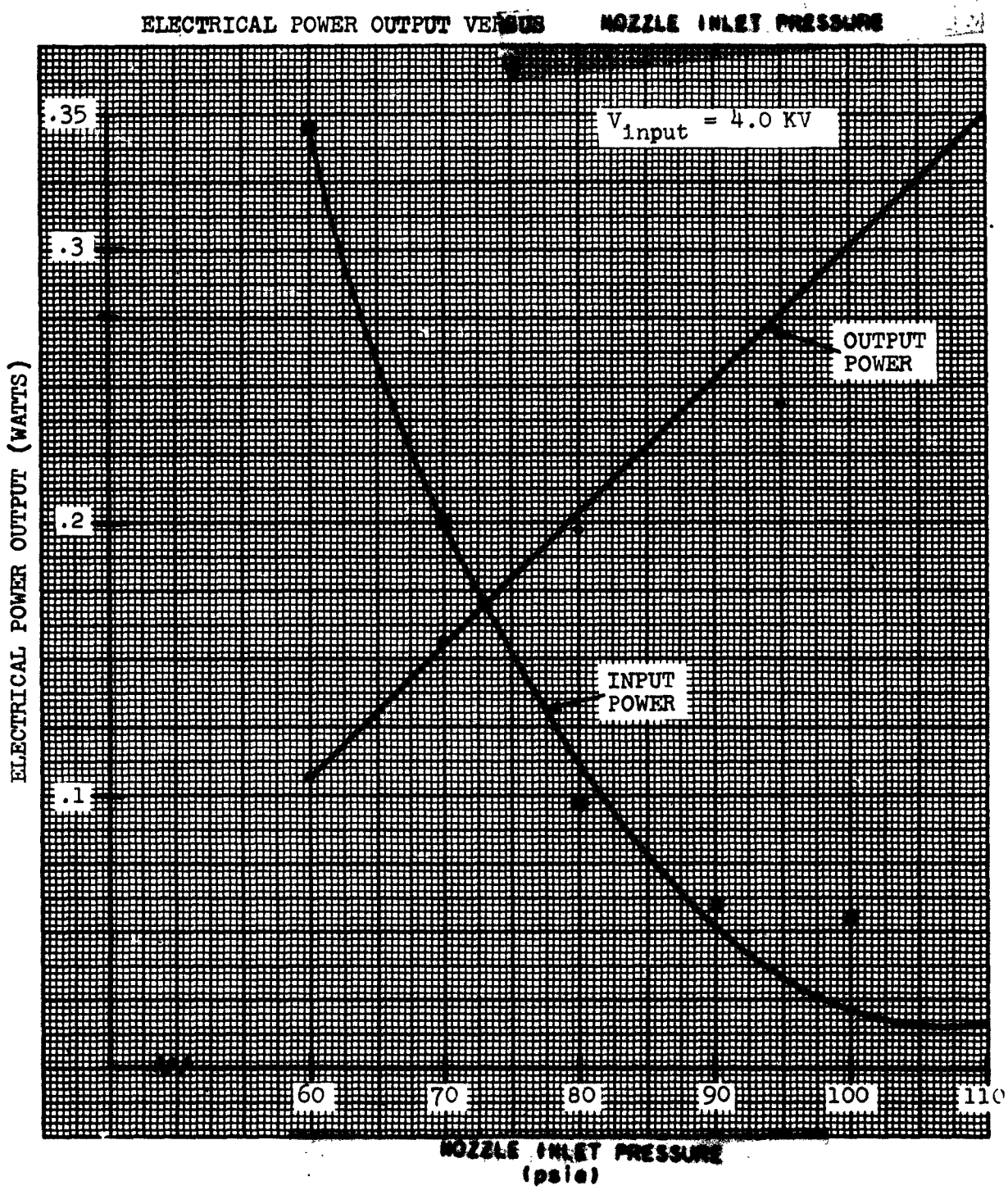

GENERATOR TEST RIG SCHEMATIC
INSTRUMENTED GENERATOR TEST SECTION

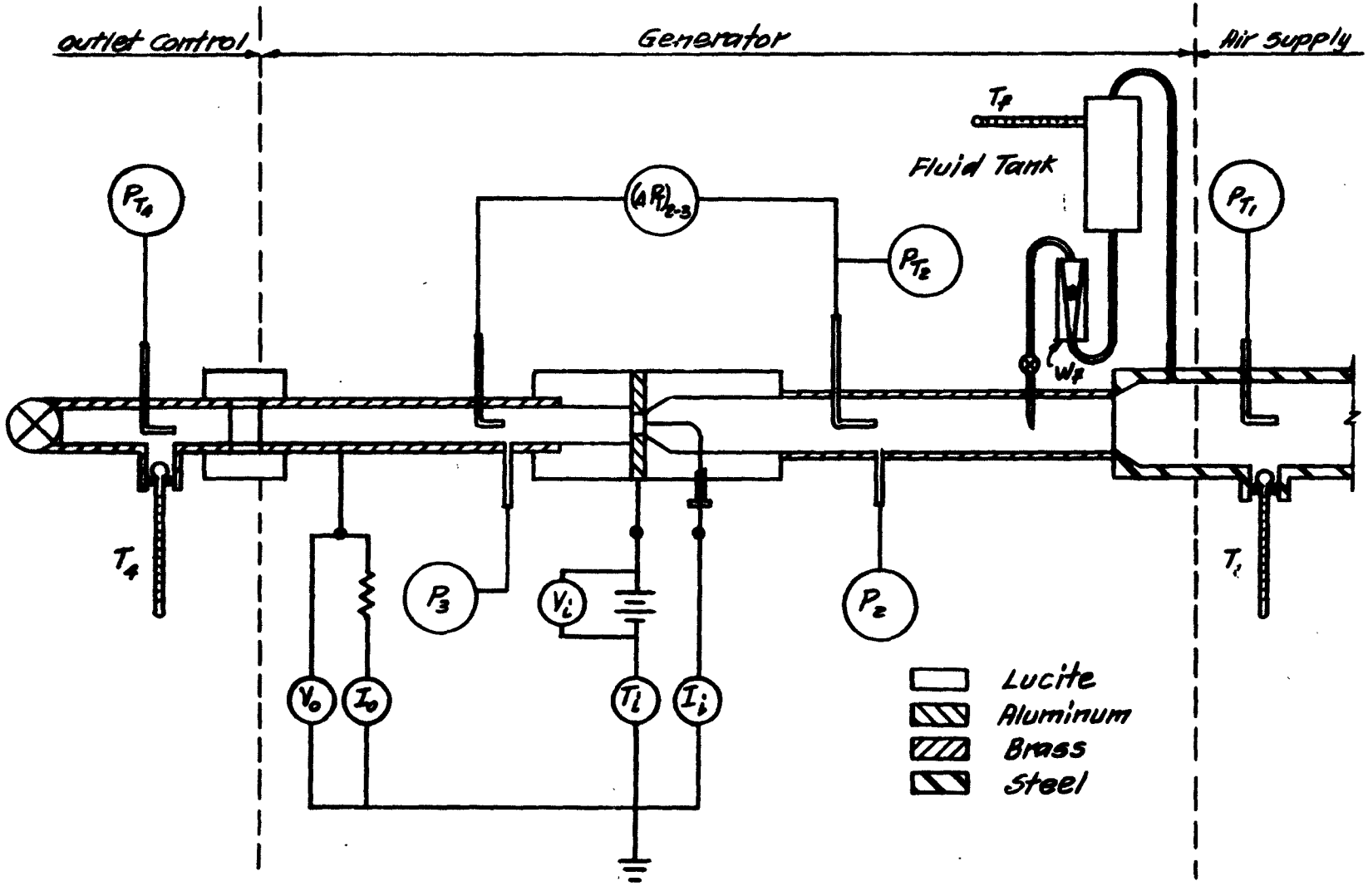

DWG # 111-7-16

FIGURE 16

DWG # 111-7-17

FIGURE 17

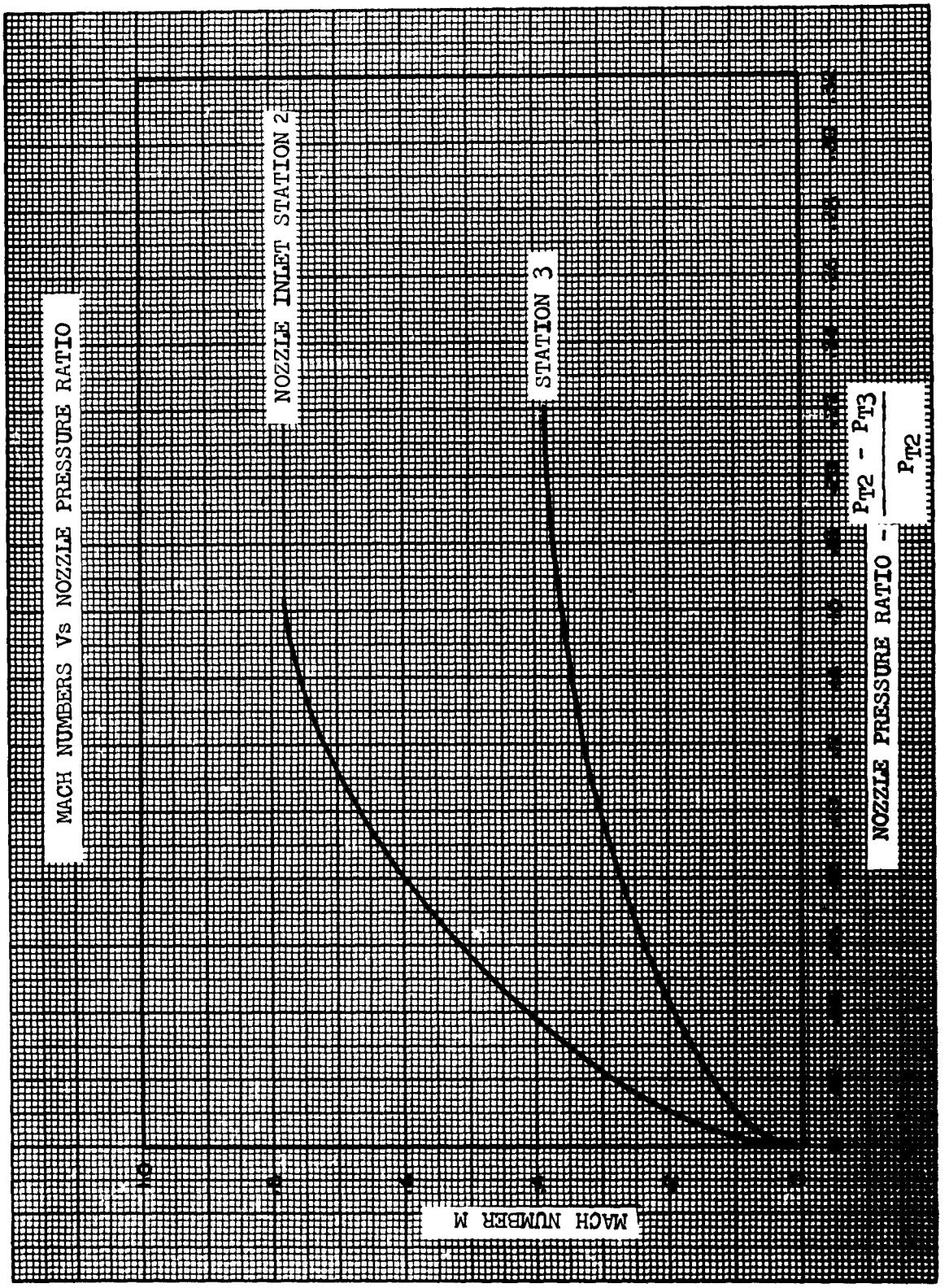

DWG # 111-7-18

FIGURE 18

ELECTRICAL POWER OUTPUT VERSUS
NOZZLE PRESSURE RATIO

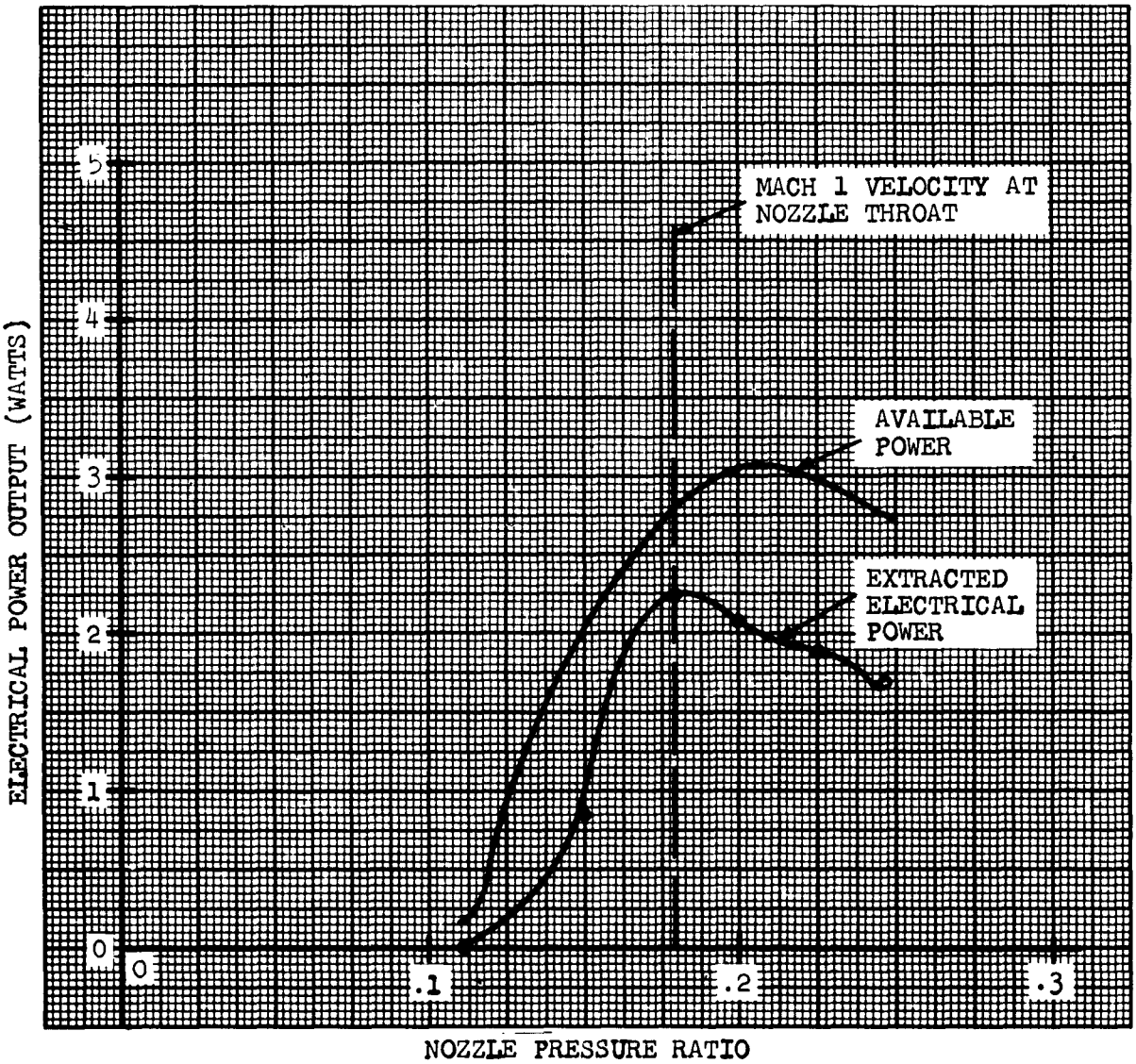

DWG # 111-7-19

FIGURE 19

CONVERSION EFFICIENCY VERSUS NORMALIZED PRESSURE DROP

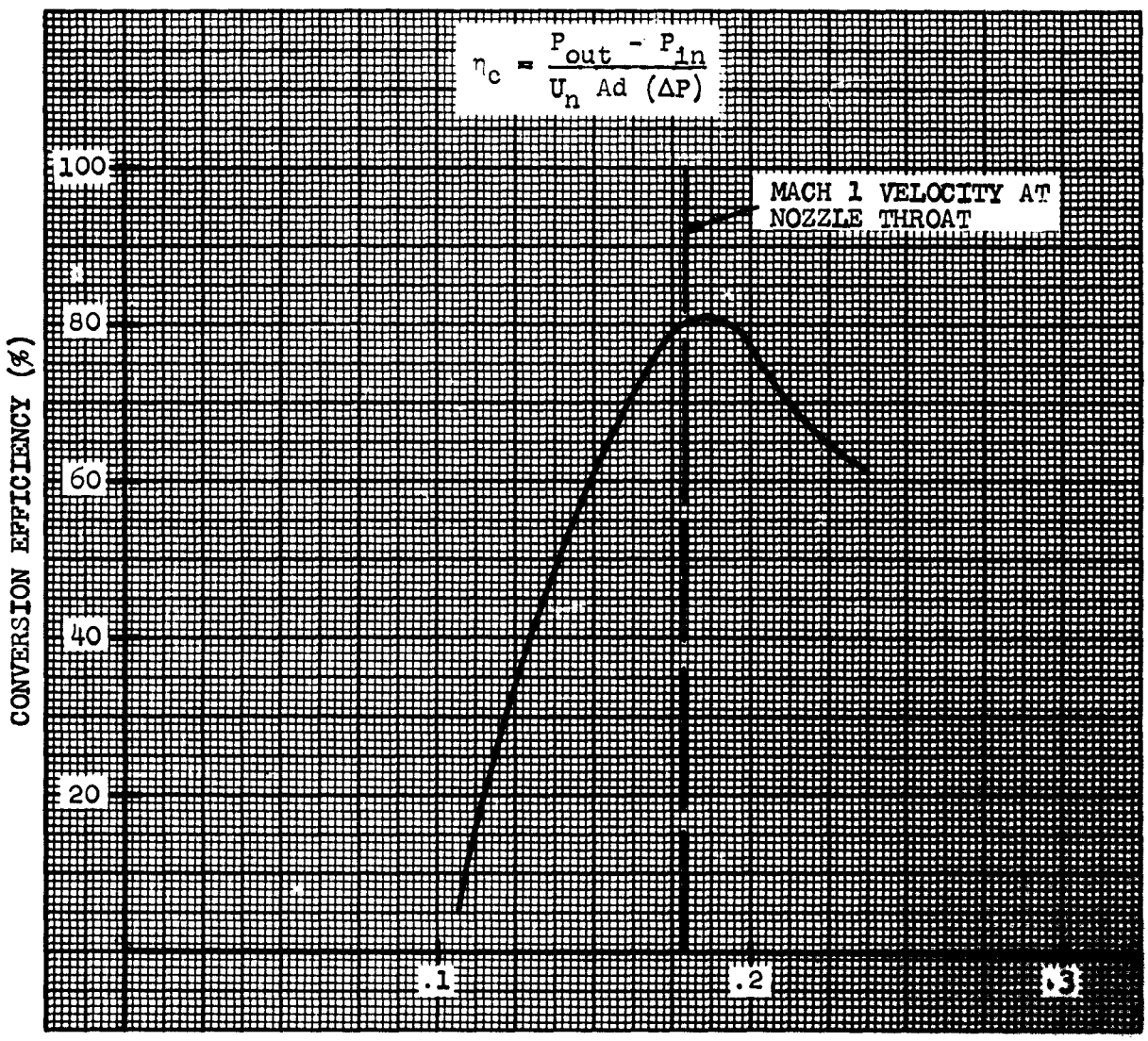

DWG # 111-7-20

FIGURE 20

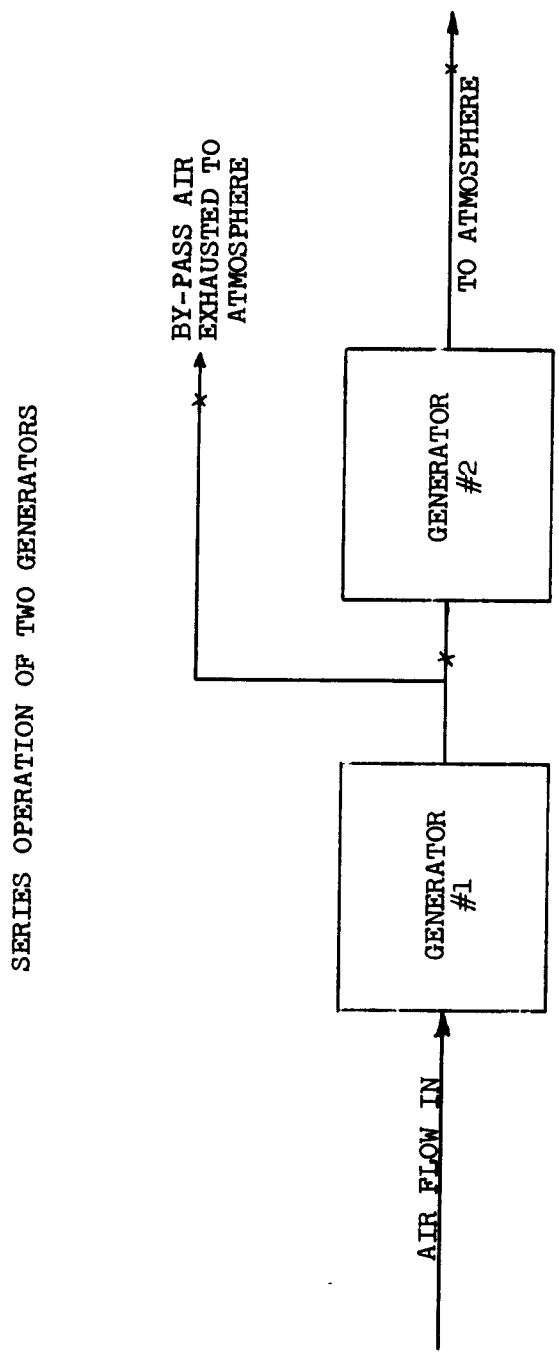

DWG # 111-7-21

FIGURE 21

ONE-HORSEPOWER REFRIGERATION UNIT SCHEMATIC

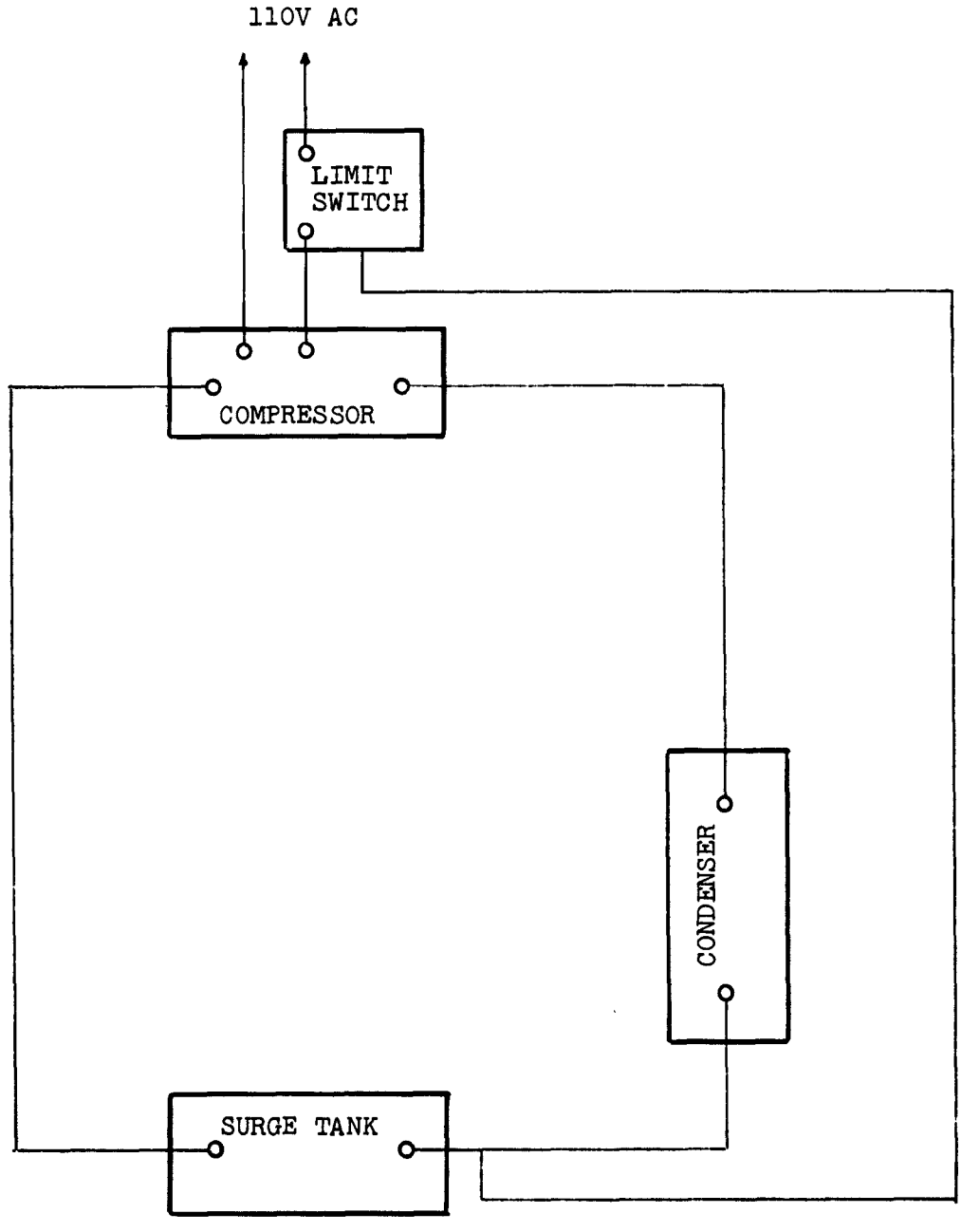

DWG # 111-7-22

FIGURE 22

CLOSED LOOP GENERATOR SYSTEM, SCHEMATIC